Original Contribution

Impairment of biliverdin reductase-A promotes brain insulin resistance in Alzheimer disease: A new paradigm

Eugenio Barone [a,b], Fabio Di Domenico [a], Tommaso Cassano [c], Andrea Arena [a], Antonella Tramutola [a], Michele Angelo Lavecchia [d], Raffaella Coccia [a], D. Allan Butterfield [e,*], Marzia Perluigi [a,*]

[a] Department of Biochemical Sciences "A. Rossi-Fanelli", Sapienza University of Rome, Piazzale A. Moro 5, 00185 Roma, Italy
[b] Universidad Autónoma de Chile, Instituto de Ciencias Biomédicas, Facultad de Salud, Avenida Pedro de Valdivia 425, Providencia, Santiago, Chile
[c] Department of Clinical and Experimental Medicine, University of Foggia, Via Napoli 20, 71122 Foggia, Italy
[d] Department of Physiology and Pharmacology "V. Erspamer", Sapienza University of Roma, Piazzale A. Moro 5, 00185 Roma, Italy
[e] Department of Chemistry, Markey Cancer Center, and Sanders-Brown Center on Aging, University of Kentucky, Lexington, KY 40506-0055, USA

ARTICLE INFO

ABSTRACT

Clinical studies suggest a link between peripheral insulin resistance and cognitive dysfunction. Interestingly, post-mortem analyses of Alzheimer disease (AD) subjects demonstrated insulin resistance in the brain proposing a role for cognitive deficits observed in AD. However, the mechanisms responsible for the onset of brain insulin resistance (BIR) need further elucidations. Biliverdin reductase-A (BVR-A) emerged as a unique Ser/Thr/Tyr kinase directly involved in the insulin signaling and represents an upstream regulator of the insulin signaling cascade. Because we previously demonstrated the oxidative stress (OS)-induced impairment of BVR-A in human AD brain, we hypothesize that BVR-A dysregulation could be associated with the onset of BIR in AD. In the present work, we longitudinally analyze the age-dependent changes of (i) BVR-A protein levels and activation, (ii) total oxidative stress markers levels (PC, HNE, 3-NT) as well as (iii) IR/IRS1 levels and activation in the hippocampus of the triple transgenic model of AD (3xTg-AD) mice. Furthermore, *ad hoc* experiments have been performed in SH-SY5Y neuroblastoma cells to clarify the molecular mechanism(s) underlying changes observed in mice. Our results show that OS-induced impairment of BVR-A kinase activity is an early event, which starts prior the accumulation of Aβ and tau pathology or the elevation of TNF-α, and that greatly contribute to the onset of BIR along the progression of AD pathology in 3xTg-Ad mice. Based on these evidence we, therefore, propose a new paradigm for which: OS-induced impairment of BVR-A is firstly responsible for a sustained activation of IRS1, which then causes the stimulation of negative feedback mechanisms (i.e. mTOR) aimed to turn-off IRS1 hyper-activity and thus BIR. Similar alterations characterize also the normal aging process in mice, positing BVR-A impairment as a possible bridge in the transition from normal aging to AD.

© 2015 Elsevier Inc. All rights reserved.

1. Introduction

During the last years a growing number of observations highlighted a close interconnection between Alzheimer disease (AD) and common diseases of modern adulthood, including obesity and type 2 diabetes mellitus (T2DM) [1,2]. Furthermore, epidemiological studies showed that hallmarks of peripheral metabolic disorders, such as glucose intolerance and/or impairment of insulin secretion, are associated with a higher risk to develop dementia or AD [2–5], whereas patients with AD more frequently present with an impaired glucose metabolism or T2DM [6,7].

This clinical evidence raised doubts about the correct functioning of insulin signaling especially in light of the neurotrophic actions mediated by insulin [8]. Indeed, the activation of insulin signaling cascade does not induce a significant glucose uptake in the brain as it does in peripheral tissues [9,10], but, rather, it modulates other important functions through the activation of the two main pathways downstream to the insulin receptor (IR): (i) the phosphoinositide-3 kinase (PI3K) pathway, which is involved in the maintenance of synaptic plasticity and memory consolidation [11,12]; and (ii) the mitogen-activated protein kinase (MAPK) cascade, which is responsible both for the induction of several genes required for neuronal and synapse growth,

* Corresponding authors.
E-mail addresses: dabcns@uky.edu (D.A. Butterfield),
marzia.perluigi@uniroma1.it (M. Perluigi).

maintenance and repair processes, as well as serving as a modulator of hippocampal synaptic plasticity that underlies learning and memory [13].

Interestingly, human postmortem studies have convincingly shown that a dysregulation of the insulin signaling with reduced downstream neuronal survival and plasticity mechanisms are consistent and fundamental abnormalities in AD [9,14,15]. In particular, AD brain is characterized by a phenomenon known as brain insulin resistance (BIR) – broadly defined as the inadequate response to insulin by target cells [13] – due to reduced insulin receptor (IR) activation and increased levels of inhibitory phosphorylation of the insulin receptor substrate-1 (IRS1) on specific serine (Ser) residues [9,14,15].

Consistent with prior studies from the Butterfield group and others [20–23], some of the common clinical signs and symptoms of T2DM and AD could arise from an impairment of the activity of biliverdin reductase-A (BVR-A). BVR-A, the main isoform of BVR [24], is a pleiotropic enzyme primarily known for its canonical activity (reductase activity) named for the reduction of heme-derived biliverdin (BV) into the powerful antioxidant and anti-nitrosative molecule bilirubin (BR) [25,26]. But BVR-A also has a unique serine/threonine/tyrosine (Ser/Thr/Tyr) kinase directly involved in insulin signaling [22,27]. Indeed, BVR-A is a direct target of IR, which stimulates BVR-A kinase activity (thereafter indicated as BVR-A activation) via Tyr phosphorylation [22]. Once activated, BVR-A is able to phosphorylate IRS1 on Ser inhibitory domains, thus representing an upstream regulator in the insulin signaling cascade [22].

We have previously reported the oxidative stress-induced impairment of BVR-A in the hippocampus of AD and amnestic mild cognitive impairment (aMCI) subjects due to reduced Tyr phosphorylation and increased 3-nitrotyrosine (3-NT) modifications, thus questioning about the real neuroprotective role of BVR-A [20,21,28]. Based on these results and given the above background, decreased BVR-A activation would have deleterious effects including the inhibition of the insulin signaling pathway.

In the present work, we longitudinally analyze the age-dependent changes of BVR-A protein levels and activation, as well as IR/IRS1 levels and activation in the hippocampus of the triple transgenic model of AD (3xTg-AD) mice, which develop both $A\beta$ and tau pathologies in an age-dependent manner [29]. The hippocampus is one of the brain regions mostly affected by amyloid beta ($A\beta$) and tau pathologies in the 3xTg-AD mice and whose alterations have major functional impact in AD symptoms. Further, we profile the molecular mechanisms responsible for the onset of BIR, by focusing on the contribution of oxidative/nitrosative stress. Our data suggest that BVR-A integrates both oxidative/nitrosative stress- and insulin-mediated signaling, both mechanisms dysregulated in AD brain.

2. Materials and methods

2.1. Animals

3, 6, 12 and 18 months-old 3xTg-AD male mice ($n=6$ per group) and their wild-type (WT) male littermates ($n=6$ per group) were used in this study. The 3xTg-AD mice harbour harbour 3 mutant human genes (APP$_{Swe}$, PS1$_{M146V}$, and tau$_{P301L}$) and have been genetically engineered by LaFerla and colleagues at the Department of Neurobiology and Behavior, University of California, Irvine [29]. Colonies of homozygous 3xTg-AD and WT mice were established at the vivarium of Puglia and Basilicata Experimental Zooprophylactic Institute (Foggia, Italy). The 3xTg-AD mice background strain is C57BL6/129SvJ hybrid and genotypes were confirmed by PCR on tail biopsies [29]. The housing conditions were controlled

(temperature 22 °C, light from 07:00–19:00, humidity 50%–60%), and fresh food and water were freely available. All the experiments were performed in strict compliance with the Italian National Laws (DL 116/92), the European Communities Council Directives (86/609/EEC). All efforts were made to minimize the number of animals used in the study and their suffering. Animals were sacrificed at the selected age and the hippocampus was extracted, flash-frozen, and stored at -80 °C until total protein extraction and further analyses were performed.

2.2. Immunohistochemistry

Briefly both 3xTg and WT mice at 3, 6, 12 and 18 months of age ($n=3$ per group, per genotype) were intra-cardioventricularly perfused with saline followed by fixation solution (4% paraformaldehyde in PBS 0.1 M, pH 7.4) at a flow rate of 36 ml min^{-1} [30]. Brains were post-fixed in the fixation solution for 1 day and then transferred in 0.02% sodium azide in PBS. Free-floating coronal sections of 50 μm thickness were obtained using a vibratome slicing system (microM, Walldorf, Germany) and stored at 4 °C in 0.02% sodium azide in PBS. The endogenous peroxidase activity was quenched for 30 min in 0.3% H_2O_2. Sections were then pretreated in 90% formic acid and incubated overnight at 4 °C either with the monoclonal 6E10 antibody (1:3000, Signet Laboratorie–Covance, Emeryville, CA, USA, #sig-39320) for $A\beta$ staining, or with the human-specific anti-tau antibody, HT7 (1:2000, Thermo Scientific Pierce Product, Rockford, IL, USA, #MN1000). After removing the primary antibody in excess, sections were incubated with the appropriate secondary antibody and developed with diaminobenzidine substrate using the avidin-biotin horseradish peroxidase system (Vector Laboratories, Inc, Burlingame, CA, USA, #SK-4100; #PK-6100). All stained slices were viewed using a Nikon 80i Eclipse microscope equipped with a DS-U1 digital camera, and NIS-elements BR software (Nikon, Tokyo, Japan). The intensity of $A\beta$ and tau immunostaining was measured semi-quantitatively as regional optical density using the Scion Image software, as previously reported [30–32]. Per each animal, measurements were obtained in at least 3 consecutive sections containing the region of interest. The averaged optical densities of non-immunoreactive regions of each section were used for background normalization.

2.3. Cell culture and treatments

The SH-SY5Y neuroblastoma cells were grown in Dulbecco's modified Eagle's medium (DMEM) supplemented with 10% fetal bovine serum (FBS), 2 mM L-glutamine, penicillin (20 units/ml) and streptomycin (20 mg/ml), (GIBCO, Gaithersburg, MD, U.S.A.). Cells were maintained at 37 °C in a saturated humidity atmosphere containing 95% air and 5% CO_2. Cells were seeded at density of 40×10^3/cm^2 in 6 wells culture dishes. After 24 h medium has been replaced with DMEM with 1% FBS and cells have been treated with (i) insulin, (ii) H_2O_2 in separate sets of experiments as following described. To test the responsiveness of our cellular model to insulin signaling the experiments have been performed as previously described with minor modifications [33]. Briefly, SH-SY5Y neuroblastoma cells were pre-treated with insulin (humulin®R, Ely-Lilly, Inadianapolis, IN, USA) 0.1 μM or vehicle (PBS) for 24 h. Insulin concentration has been selected based on previous reports [22,33]. Then, medium was discarded, cells were washed twice with PBS, and rechallenged with DMEM with 1% FBS containing insulin (0.1–0.5–1–5 μM) or vehicle (PBS) for an additional hour to mimic insulin over-exposure. To test the effects of oxidative/nitrosative stress on the insulin signaling, cells have been treated with peroxynitrite (ONOO$^-$, 50–500 μM) or hydrogen peroxide (H_2O_2, 1–50 μM) (Sigma-Aldrich, St Louis, MO, USA, #16911) or vehicle (PBS) for 24 h. To test the effects produced by

the silencing of BVR-A on the insulin signaling, SH-SY5Y neuro-blastoma cells were seeded at density of $40 \times 10^3/cm^2$ in 6 wells culture dishes. After 24 h medium has been replaced with DMEM with 1% FBS, without antibiotics. Following, cells have been treated in parallel with insulin (0.1 μM), transfected with 25pmol of a small-interfering RNA (siRNA) for BVR-A (Ambion, Life Technologies, LuBioScience GmbH, Lucerne, Switzerland, #4392420) using Lipofectamine® RNAiMAX reagent (Invitrogen, Life Technologies, LuBioScience GmbH, Lucerne, Switzerland, #13778-030) according to the manufacturer's protocol, or co-treated with insulin (0.1 μM) and BVR-A siRNA for 24 h. At the end of each treatment, cells were washed twice with PBS, collected and proteins were extracted as described below.

2.4. Samples preparation

Total protein extracts were prepared in RIPA buffer (pH 7.4) containing Tris-HCl (50 mM, pH 7.4), NaCl (150 mM), 1% NP-40, 0.25% sodium deoxycholate, EDTA (1 mM), 0.1% SDS, supplemented with proteases inhibitors [phenylmethylsulfonyl fluoride (PMSF, 1 mM), sodium fluoride (NaF, 1 mM) and sodium orthovanadate (Na_3VO_4, 1 mM)]. Before clarification, hippocampal tissues were homogenized by 20 passes with a Wheaton tissue homogenizer. Both hippocampal tissues homogenates and collected cells were clarified by centrifugation for 1 h at $16,000 \times g$, 4 °C. The supernatant was then extracted to determine the total protein concentration by the Bradford assay (Pierce, Rockford, IL).

2.5. Slot Blot analysis

For total Protein Carbonyls (PC) levels: hippocampal total protein extract samples (5 μl), 12% sodium dodecyl sulfate (SDS; 5 μl), and 10 μl of 10 times diluted 2,4- dinitrophenylhydrazine (DNPH) from 200 mM stock were incubated at room temperature for 20 min, followed by neutralization with 7.5 μl neutralization solution (2 M Tris in 30% glycerol) and then loaded onto nitrocellulose membrane as described below.

For total (i) protein-bound 4-hydroxy-2-nonenals (HNE) and (ii) 3-nitrotyrosine (3-NT) levels: hippocampal total protein extract samples (5 μl), 12% SDS (5 μl), and 5 μl modified Laemmli buffer containing 0.125 M Tris base, pH 6.8, 4% (v/v) SDS, and 20% (v/v) glycerol were incubated for 20 min at room temperature and then loaded onto nitrocellulose membrane as described below.

Proteins (250 ng) were loaded in each well on a nitrocellulose membrane under vacuum using a slot blot apparatus. The membrane was blocked in blocking buffer (3% bovine serum albumin) in PBS 0.01% (w/v) sodium azide and 0.2% (v/v) Tween 20 for 1 h and incubated with an anti-2,4-dinitrophenylhydrazone (DNP) adducts polyclonal antibody (1:100, EMD Millipore, Billerica, MA, USA, #MAB2223) or HNE polyclonal antibody (1:2000, Novus Biologicals, Abingdon, United Kingdom, #NB100-63093) or an anti 3-NT polyclonal antibody (1:1000, Santa Cruz, Santa Cruz, CA, USA, #sc-32757) in PBS containing 0.01% (w/v) sodium azide and 0.2% (v/v) Tween 20 for 90 min. The membrane was washed in PBS following primary antibody incubation three times at intervals of 5 min each. The membrane was incubated after washing with an anti-rabbit IgG alkaline phosphatase secondary antibody (1:5000, Sigma-Aldrich, St Louis, MO, USA) for 1 h. The membrane was washed three times in PBS for 5 min each and developed with Sigma fast tablets (5-bromo-4-chloro-3-indolyl phosphate/nitro-blue tetrazolium substrate [BCIP/NBT substrate]). Blots were dried, acquired with Chemi-Doc MP (Bio-Rad, Hercules, CA, USA) and analyzed using Image Lab software (Bio-Rad, Hercules, CA, USA). No non-specific binding of antibody to the membrane was observed.

2.6. Western blot

For western blots, 30 μg of proteins were resolved on 12% and 7.5% SDS–PAGE using Criterion Gel TGX (Bio-Rad, Hercules, CA, USA). Before imunoblot analysis the gel image analyzed for total protein load was acquired to then normalize blot analysis. For immunoblot analysis, gels were transferred onto nitrocellulose membranes (Bio-Rad, Hercules, CA, USA) and membranes were blocked with 3% bovine serum albumin in 0.5% Tween-20/Tris-buffered saline (TTBS) and incubated overnight at 4 °C with the following antibodies: anti-BVR-A (1:5000, abcam, Cambridge, United Kingdom, #ab90491), anti-BVR-A (1:1000, Sigma-Aldrich, St Louis, MO, USA, #B8437), anti-IRβ (1:1000, Cell Signaling, Bioconcept, Allschwill, Switzerland, #3020), anti-phospho(Tyr1162/1163)-IRβ (1:500, Santa Cruz, Santa Cruz, CA, USA, #sc-25103), anti-IRS1 (1:1000, Cell Signaling, Bioconcept, Allschwill, Switzerland, #3407), anti-phospho(Ser307)-IRS1 (1:500, Cell Signalling, Bioconcept, Allschwill, Switzerland, #2381), anti-phospho(Tyr632)-IRS1 (1:500, Santa Cruz, Santa Cruz, CA, USA, #sc-17196), anti-mTOR (1:1000, Cell Signaling, Bioconcept, Allschwill, Switzerland, #2983), anti-phospho(Ser2448)-mTOR (1:500, Cell Signaling, Bioconcept, Allschwill, Switzerland, #5536), anti-HO1 (1:1000, Enzo Life Sciences, Farmingdale, NY, USA, #ADI-SPA-895), anti-TNF-α (1:1000, EMD Millipore, Billerica, MA, USA, #AB1837P), anti-phospho-Tyrosine (1:2000, Cell Signaling, Bioconcept, Allschwill, Switzerland, #9416), anti-3NT (1:500, Santa Cruz, Santa Cruz, CA, USA, #sc-32757). After 3 washes with TTBS the membranes were incubated for 60 min at room temperature with anti-rabbit/mouse/goat IgG secondary antibody conjugated with horseradish peroxidase (1:5000; Sigma-Aldrich, St Louis, MO, USA). Membranes were developed with the Super Signal West Pico chemiluminescent substrate (Thermo Scientific, Waltham, MA, USA), acquired with Chemi-Doc MP (Bio-Rad, Hercules, CA, USA) and analyzed using Image Lab software (Bio-Rad, Hercules, CA, USA) that permits the normalization of a specific protein signal with the β-actin signal in the same lane or total proteins load.

2.7. Immunoprecipitation

The immunoprecipitation procedure was performed as previously described [34], with minor modifications. Briefly, 150 μg of proteins were dissolved in 500 μL of RIPA buffer (10 mM Tris, pH 7.6; 140 mM NaCl; 0.5% NP-40) supplemented with proteases inhibitors and incubated with 1 μg anti-BVR-A polyclonal antibody at 4 °C overnight. Immunocomplexes were collected using protein A/G suspension for 2 h at 4 °C and washed 5 times with immunoprecipitation buffer. Immunoprecipitated BVR-A was recovered by re-suspending the pellets in reducing sodium dodecyl sulfate buffers and electrophoresing them on 12% gels, followed by western blot analysis. Total BVR-A was used as a loading control as previously described [20,21,35,36].

2.8. BVR-A reductase activity

We determined BVR-A activity in hippocampal tissues extracted from both 3xTg-AD and WT mice using a BVR assay kit (Sigma-Aldrich, St Louis, MO, USA #CS1100) as per manufacturer's instructions with minor modification. Briefly, 150 μg of proteins were prepared for the assay and loaded in the 96 well plates. BVR positive control solution (2.5, 5, 10, 15 20 μL) was included in the assay for generation of a standard curve. Fifty microliters assay buffer and 150 μL working solution (containing NAPDH, substrate solution and assay buffer) were added to each standard and sample on the plate. The plate was placed on the UV–vis plate reader at 37 °C and read every minute for 10 min. The reading at 5 min had a linear reaction rate, and was chosen for BVR activity
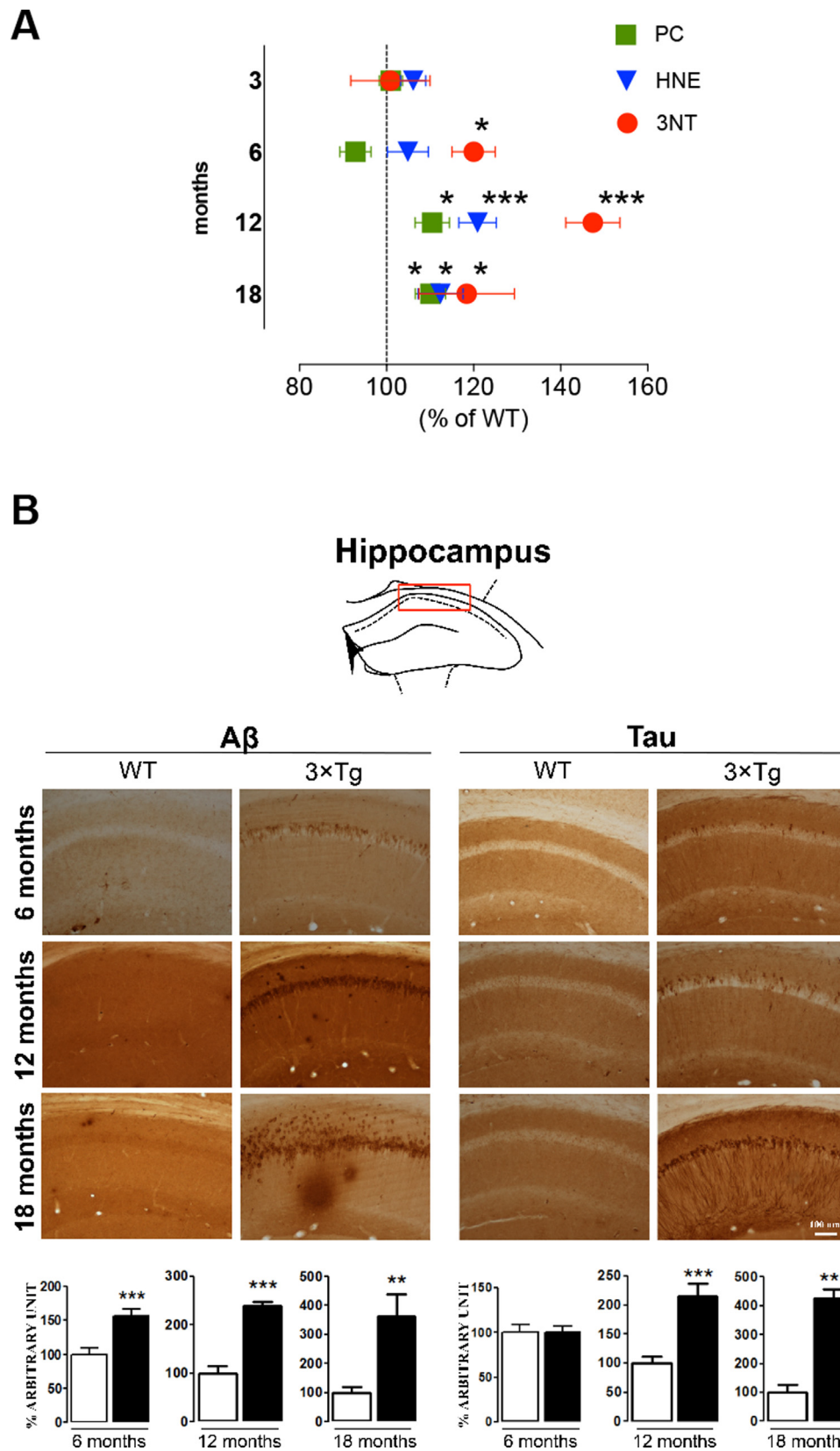
Fig. 1. Increased oxidative and nitrosative stress levels progresses with AD pathology in the hippocampus of 3xTg-AD mice. (A) Protein carbonyls (PC) levels (green squares), protein-bound 4-hydroxy-2-nonenal (HNE) levels (blue triangles) and 3-nitrotyrosine (3-NT) levels (red dots) evaluated in the hippocampus of 3xTg-AD mice at 3 ($n=6$), 6 ($n=6$), 12 ($n=6$) and 18 ($n=6$) months of age. Densitometric values shown are given as percentage of the age-matched WT mice ($n=6$/group), set as 100%. Means $\pm$ SEM of three replicates of each individual sample per group. $^{*}p < 0.05$ and $^{**}p < 0.01$ versus WT (Student's t-test). (B) Representative microphotographs (10 $\times$ magnification, scale bar 100 μm) and results obtained from the semi-quantitative analyses of Aβ and tau immunostaining from WT ($n=3$, white bars) and 3xTg-AD ($n=3$, black bars) mice. The red square within the brain diagram illustrates the site where the representative microphotographs were taken. The data are mean $\pm$ SEM $^{**}p < 0.01$ and $^{***}p < 0.001$ versus age-matched WT mice (Unpaired Student's t-test, $n=3$).

calculations. Values are expressed as Unit (U)/mL [Unit definition as per manufacturer's instruction: 1 unit of BVR will transform 1 nanomole of biliverdin to bilirubin in an NADPH dependent reaction at pH 8.5 at 37 °C].

2.9. Statistical analyses

All data are presented as means $\pm$ SEM of n independent samples per group. Student's t test or a nonparametric one-way ANOVA with post hoc Turkey's t –tests were applied for statistical analysis. $p < 0.05$ was considered significantly different from the reference value.
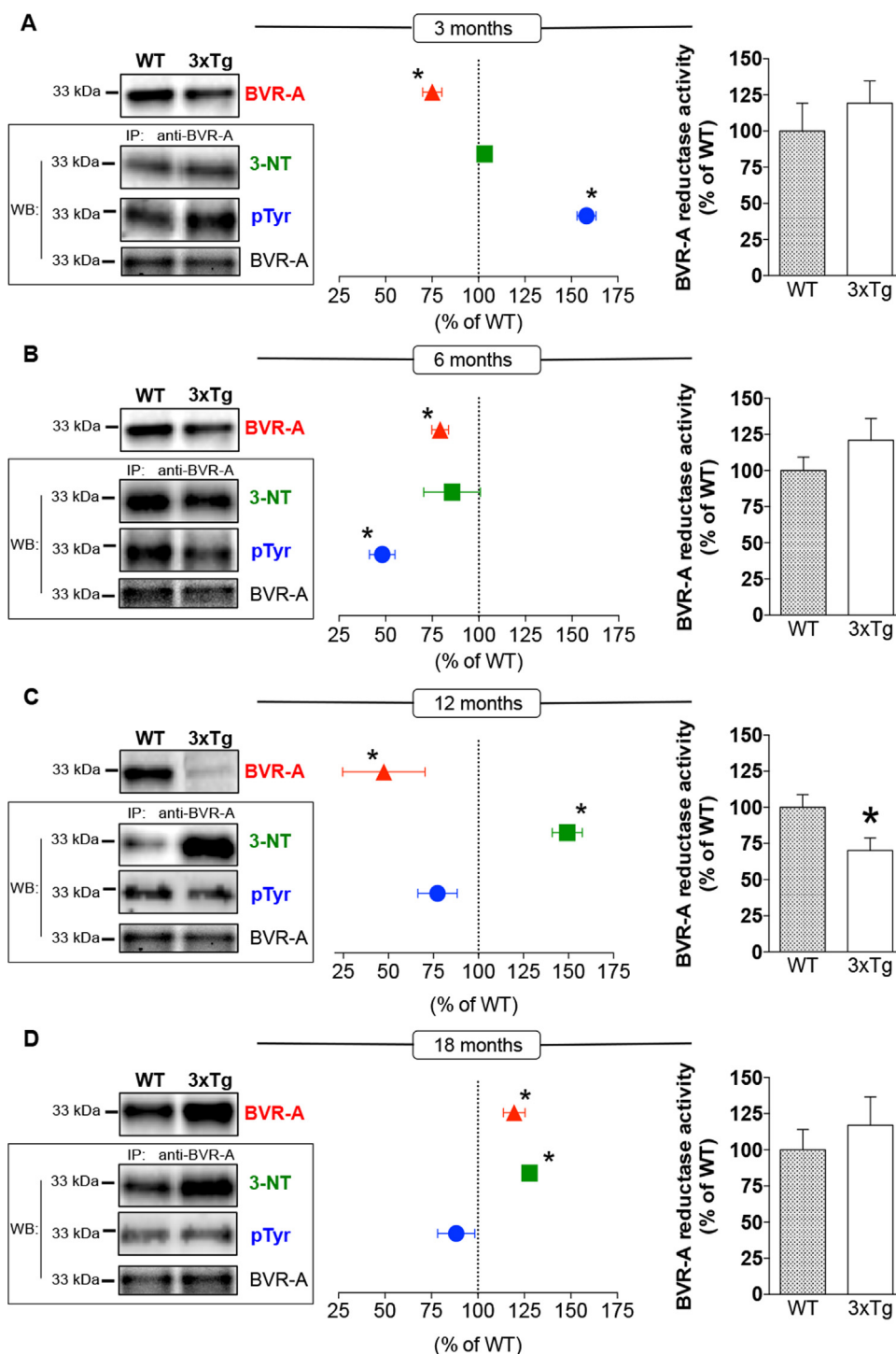
Fig. 2. Early impairment of BVR-A is observed during the progression of AD pathology in the hippocampus of 3xTg-AD mice. BVR-A (i) protein levels (red triangles), (ii) 3-nitrotyrosine (3-NT) modifications (green squares), (iii) Tyr phosphorylation (pTyr) (blue dots) and (iv) reductase activity (right columns) evaluated in the hippocampus of 3xTg-AD mice at (A) 3 ($n=6$), (B) 6 ($n=6$), (C) 12 ($n=6$) and (D) 18 ($n=6$) months of age. *Left panels:* western blot analyses. Representative bands are shown. *Middle panels:* densitometric analyses of western blot protein bands. BVR-A protein levels were normalized per total protein load. 3-NT modifications and pTyr levels on BVR-A were normalized by using total BVR-A as loading control [35,36]. Densitometric values shown are given as percentage of WT mice ($n=6$/group) set as 100%. *Right panels:* BVR-A reductase activity expressed as percent of WT mice ($n=6$/group) and evaluated as described in Materials and Methods. Means $\pm$ SEM, *$p < 0.05$ *vs* WT mice (Student's t-test).

3. Results

3.1. Oxidative stress correlates with AD pathology in 3xTg-AD mice

Based on our previous results about oxidative/nitrosative stress-induced BVR-A impairment in human AD and aMCI brain [20,21,37] and considering the regulatory role exerted by BVR-A on IRS1 [22] we hypothesized that increased levels of oxidative stress in our AD model target BVR-A affecting its function and resulting in the impairment of the insulin signaling as observed in AD patients. In order to decipher the contribution of increased oxidative and/or nitrosative stress levels to the potential alterations of BVR-A function, we initially characterized for the first time the age-associated modifications of the oxidative/nitrosative stress markers in the 3xTg-AD mice. We therefore evaluated changes of total protein carbonyls (PC), total 4-hydroxy-2-nonenal adducts (HNE) and total 3-nitrotyrosine (3-NT) levels in the hippocampus of 3xTg-AD mice with respect to the appropriate WT littermate controls at 3, 6, 12 and 18 months of age. Interestingly, we found a significant elevation of 3-NT levels at 6 months of age, which further rises at 12 months and remains still elevated at 18 months (Fig. 1A). In addition, a significant elevation of both PC and HNE adducts is evident both at 12 and 18 months of age (Fig. 1A). Furthermore, age-associated significant changes also are evident in the hippocampus of 3xTg-AD mice (see Supplementary Fig. 1)

These changes correlate with the neuropathological AD alterations occurring in the same time-frame in the hippocampus of 3xTg-AD mice (Fig. 1B). Three-month-old 3xTg-AD mice have no detectable neuropathological alterations in the brain, as previously demonstrated [38]. As the 3xTg-AD mice age, they gradually accumulate Aβ and tau pathology in their brains. Specifically, 6-month old 3xTg-AD mice showed a significant increase in Aβ immunostaining compared to age-matched WT mice, while no difference was found in tau immunoreactivity at this age in the hippocampus. At 12 months of age 3xTg-AD mice showed Aβ deposits and human tau-reactive neurons in the hippocampus. Finally, we found dense Aβ deposit and extensive human tau immunoreactivity in the 18-month old 3xTg-AD mice. None of these immunoreactive structures were detected in the WT brains (Fig. 1B).

3.2. The impairment of BVR-A occurs early in the 3xTg-AD mice

To unravel the contribution of increased oxidative/nitrosative stress levels to the hypothesized impairment of BVR-A in our AD model, we first analyzed changes of BVR-A protein levels, activation (pTyr-BVR-A) and oxidative stress-induced post-translational modifications (3-NT-BVR-A).

A significant reduction of BVR-A protein levels occurs from 3 to 12 months in the hippocampus of 3xTg-AD mice with respect to WT mice, whereas a significant increase was observed at 18 months (Fig. 2). With regard to BVR-A activation, we observed a significant increase at 3 months, followed by a drastic reduction at 6 months of age. Both at 12 and 18 months of age, we still observed a reduction of pTyr-BVR-A in the 3xTg-AD mice compared to WT group, although did not reach the statistical significance (~25% and ~20%, respectively at 12 and 18 months of age, Fig. 2). At these time-points (corresponding to the advanced stages of AD pathology in the hippocampus), the altered BVR-A activation was paired to a significant increase of 3-NT modifications on the BVR-A in the 3xTg-AD mice compared to WT group. In particular, the 3-NT modifications on the BVR-A peaked at 12 months, reaching 150% in the 3xTg-AD mice compared to the relative control group. Furthermore, we investigated whether BVR-A reductase activity was also impaired as reported in human AD brain [21]. Indeed, the reductase activity was significantly reduced only at 12 months

coincidently with the maximal increase of 3-NT-BVR-A at this time point, which is probably responsible of a general impairment of the protein (Fig. 2). All together, while the results obtained at 12 and 18 months of age recapitulate our previous observations in human AD brains [20,21], data collected at 3 and 6 months of age provide novel lines of evidence about the early dysregulation of BVR-A either in terms of protein levels or activity, which worsen with the progression of AD pathology in these mice. The reduction of BVR-A activation paralleled increased total oxidative/nitrosative stress levels from 6 to 18 months, thus suggesting a link between these events during the progression of AD pathology.

## 3.3. BVR-A impairment leads to BIR in the 3xTg-AD mice

As noted above BVR-A was impaired early in 3xTg-AD mice hippocampus associated with increased oxidative/nitrosative stress levels. Accordingly, we evaluated changes with regard to IR and IRS1 protein levels/activation in the hippocampus of 3xTg-AD mice at 3, 6, 12 and 18 months of age. These analyses shed light on the IR and IRS1 age-associated alterations and aim to investigate the mechanisms through which the BVR-A dysregulation might impact insulin signaling in AD. The evaluation of IR protein levels and activation [pIR$^{(Tyr1662/1163)}$] as well as IRS1 protein levels and both activation [pIRS1$^{(Tyr632)}$] and inactivation [pIRS1$^{(Ser307)}$] markers in the hippocampus of 3xTg-AD mice highlighted two distinct phases (3-6 and 12-18 months). The first interesting result appears to be the significant reduction of IR protein levels (Fig. 3A), observed in hippocampus from 3-months old 3xTg-AD mice, which is associated with a consistent elevation of IR activation (Fig. 3A) without significant changes of IRS1 protein levels or activation (Fig. 3A). At 6 months of age, both IR and IRS1 protein levels are reduced, while they appear to be consistently activated (Fig. 3B). At 12 months of age, we observed a completely opposite scenario characterized by a reduction of IR protein levels and activation (Fig. 3C) together with a consistent increase of IRS1 inactivation (Fig. 3C), supporting the onset of a state of BIR. Finally, at 18 months of age, 3xTg-AD mice are characterized by a persistent state of BIR as demonstrated by the elevated levels of IRS1 Ser307 phosphorylation (Fig. 3D). These results are particularly intriguing because they allow us to identify different phases along the progression of AD pathology, which finally led to insulin resistance in the hippocampus of 3xTg-AD mice. Noteworthy, the consistent increase of IRS1 activation is associated with the strong reduction of BVR-A activation at 6 months of age, whereas the persistent impairment of BVR-A at 12 months is associated with a clear inactivation of IRS1. These evidences are in agreement with our hypothesis suggesting that the lack of control exerted by BVR-A on IRS1 is firstly associated with IRS1 hyperactivation, which in turn leads to BIR probably through feedback mechanisms aimed to turn-off IRS1 hyperactivity.

3.4. BVR-A impairment precedes TNF-α elevation in the 3xTg-AD mice

Because TNF-α is known to inhibit BVR-A promoter activity [39] and TNF-α is also considered one of the most conceivable mediators of BIR in AD [18] we wondered whether reduced BVR-A protein levels could result from increased TNF-α in the hippocampus of 3xTg-AD mice. We found a significant reduction of TNF-α levels from 3 to 12 months of age followed by a consistent increase at 18 months in the hippocampus of 3xTg-AD mice with respect to WT (Fig. 4). These results agrees with previous data showing reduced microglia activation at 6 months [40] and increased TNF-α mRNA levels at 16 months of age [41] and possibly indicate that reduction BVR-A protein levels are independent from TNF-α and occurs even before TNF-α elevation during the
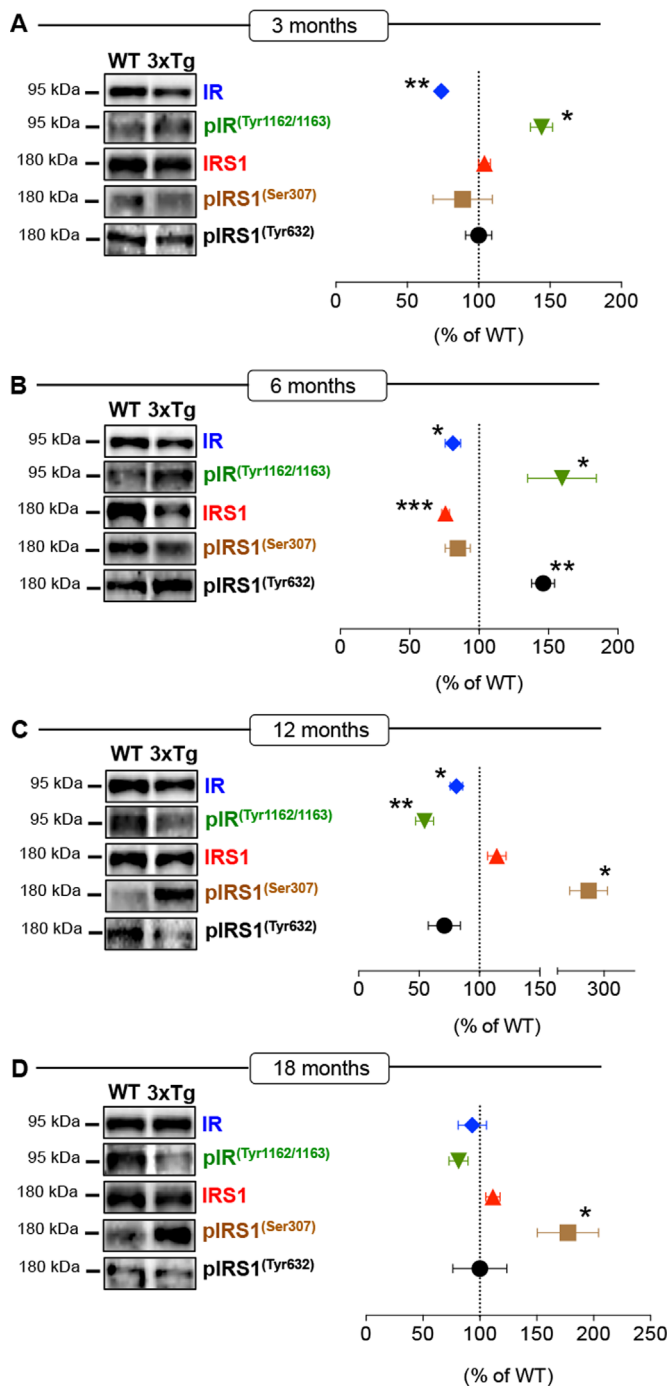
Fig. 3. Hyper-activation of the insulin signaling precedes BIR in the hippocampus of 3xTg-AD mice. IR protein levels (blue diamonds), IR activation [pIR$^{(Tyr1162/1163)}$, green triangles], IRS1 protein levels (red triangles), IRS1 inactivation [pIRS1$^{(Ser307)}$, brown squares] and IRS1 activation [pIRS1$^{(Tyr632)}$, black dots] evaluated in the hippocampus of 3xTg-AD mice at (A) 3 ($n=6$), (B) 6 ($n=6$), (C) 12 ($n=6$) and (D) 18 ($n=6$) months of age. *Left panels:* western blot analyses. Representative bands are shown. *Right panels:* densitometric analyses of western blot protein bands. Protein levels were normalized per total protein load. IR- and IRS1-associated phosphorylations were normalized by taking into account the respective protein levels and are expressed as the ratio between the phosphorylated form and the total protein levels: pIR$^{(Tyr1162/1163)}$/IR, pIRS1$^{(Ser307)}$/IRS1 and pIRS1$^{(Tyr632)}$/IRS1. Densitometric values shown are given as percentage of WT mice ($n=6$/group) set as 100%. Means $\pm$ SEM, $^{*}p < 0.05$, $^{**}p < 0.01$ and $^{***}p < 0.001$ *vs* WT mice (Student's t-test). (For interpretation of the references to color in this figure legend, the reader is referred to the web version of this article.)
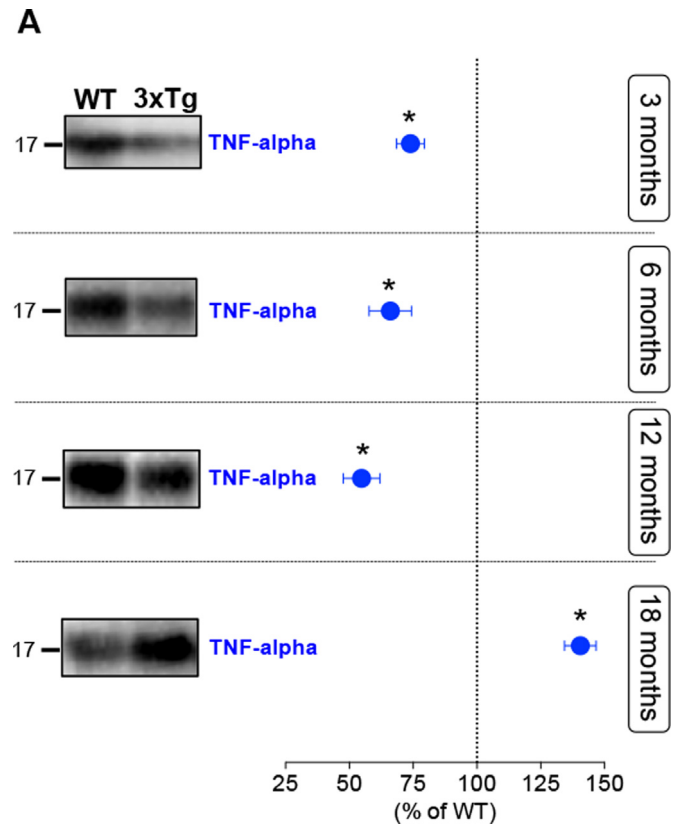

Fig. 4. Age-associated changes of TNF-α protein levels in the hippocampus of 3xTg-AD. TNF-α protein levels (blue dots) in the hippocampus of 3xTg-AD mice at 3 ($n=6$), 6 ($n=6$) and 12 ($n=6$) and 18 ($n=6$) months of age. *Left panels:* western blot analyses. Representative bands are shown. *Right panels:* densitometric analyses of western blot protein bands. TNF-α protein levels were normalized per total protein load. Densitometric values shown are given as percentage of WT mice ($n=6$/group) set as 100%. Means $\pm$ SEM, $^{*}p < 0.05$ *vs* WT mice (Student's t-test). (For interpretation of the references to color in this figure legend, the reader is referred to the web version of this article.)

progression of AD pathology in 3xTg-AD mice.

3.5. BVR-A impairment and BIR in normal aging

In order to identify whether BIR occurring during normal aging was associated with a dysregulation of BVR-A, we then analyzed changes of IR/IRS1 protein levels and activation in light of the changes occurring with regard to BVR-A in the hippocampus of WT mice aged from 3 to 18 months. We found a reduction of BVR-A protein levels both at 12 and 18 months (Fig. 5A). A reduction of BVR-A activation was also observed although this value did not reach statistical significance (Fig. 5A). Furthermore, 18-month old WT mice exhibit a significant increase of 3-NT-BVR-A (Fig. 5A) together with a significant decrease of BVR-A reductase activity (see Supplementary Fig. 2A), thus supporting a general age-associated impairment of the protein. Increased BVR-A nitration in the hippocampus of the aged mice parallels the increase of the oxidative/nitrosative stress levels at the same age (see Supplementary Fig. 2B). With regard to TNF-α levels, the hippocampus of WT mice was characterized by a significant increase at 12 months followed by a consistent reduction at 18 months (see Supplementary Fig. 2C). The analysis of IR protein levels did not reveal any significant change (Fig. 5B), whereas with regard to IR activation we found a consistent increase from 3 to 12 months, followed by a fall at 18 months (Fig. 5B). A decrease of IRS1 protein levels together with a consistent IRS1 inactivation with age has been found (Fig. 5B). Indeed, while at 6 months of age increased IR activation
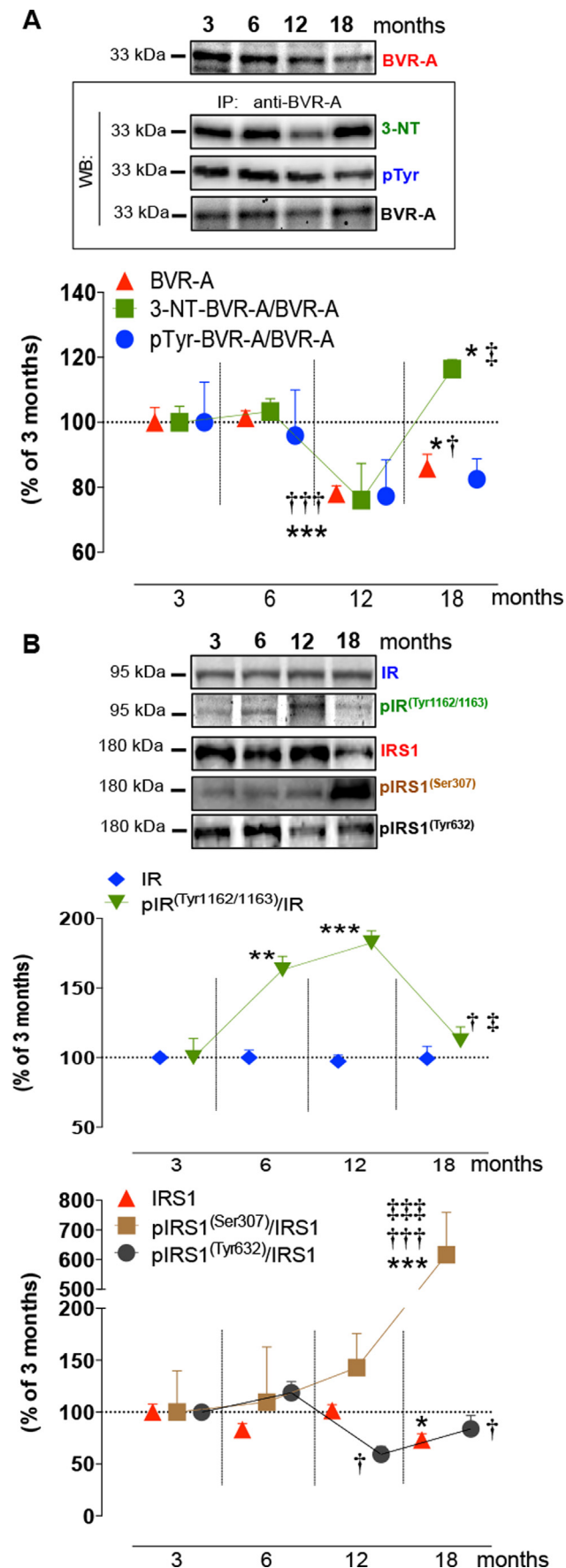
is not associated with IRS1 hyperactivation probably because BVR-A is still functioning; at 12 and 18 months of age, reduced BVR-A protein levels and activation are associated with the inactivation of IRS1, and thus BIR. These results recall what we have observed in 3xTg-AD mice and suggest that the impairment of BVR-A could represent a bridge in the transition from normal aging to AD.

3.6. BVR-A impairment is associated with BIR in SH-SY5Y neuroblastoma cells

Changes observed in the hippocampus during both AD and normal aging strongly suggest that BVR-A exerts an up-stream control on IRS1 aimed to regulate the fate of insulin signaling. In order to demonstrate that the inactivation of BVR-A is effectively a central event in the onset of BIR we first reproduced a condition of BIR in vitro to evaluate changes with regard to IR/IRS1 and BVR-A. For an easier comprehension of the results obtained in SH-SY5Y neuroblastoma cells, we will refer to BIR also thereafter. In a preliminary set of experiments, we investigated whether insulin 0.1 μM administered for 24 h was able to activate the insulin signaling and whether the administration of additional increasing doses of insulin (0.1–5 μM for 1 h) aimed to mimic insulin over-exposure would promote BIR in our cellular model. As expected, insulin pre-treatment (0.1 μM for 24 h) promotes a significant increase of both IR and IRS1 activation (Fig. 6A and see Supplementary Fig. 3). By re-challenging pre-treated cells with increasing doses of insulin (0.1–5 μM), we observed two opposite effects: increased IRS1 inactivation with insulin 0.1 μM and 0.5 μM (Fig. 6A and see Supplementary Fig. 3) and increased IRS1 activation with insulin 5 μM (Fig. 6A and see Supplementary Fig. 3). Interestingly, none of these conditions were characterized by changes of BVR-A protein levels (see Supplementary Fig. 3). However, based on our hypothesis, the evaluation of BVR-A activation, rather than its expression levels, would provide more information about the molecular mechanisms underlying insulin-mediated effects. We therefore selected 3 points representative of 3 different conditions, i.e., normal insulin signaling (Ins 0.1 μM for 24 h), BIR (Ins 0.1 μM for 24 h+Ins 0.1 μM for 1 h) and the over-induced insulin signaling (Ins 0.1 μM for 24 h+Ins 5 μM for 1 h) to characterize BVR-A activation in these different situations. As shown in Fig. 6A, normal insulin signaling is associated with a significant increase of pTyr-BVR-A as expected, whereas BIR is characterized by a reduction of BVR-A activation (Fig. 6A). Surprisingly, Ins 5 μM for 1 h, which

Fig. 5. BVR-A impairment parallels BIR during normal aging in the hippocampus of WT mice. (A) BVR-A (i) protein levels (red triangles), (ii) 3-nitrotyrosine (3-NT) modifications (green squares) and (iii) Tyr phosphorylation (pTyr) (blue dots) evaluated in the hippocampus of WT mice at 3 ($n=6$), 6 ($n=6$), 12 ($n=6$) and18 ($n=6$) months of age. Upper panels: western blot analyses. Representative bands are shown. Lower panels: densitometric analyses of western blot protein bands. BVR-A protein levels were normalized per total protein load. 3-NT modifications and pTyr levels on BVR-A were normalized by using total BVR-A as loading control [35,36]. (B) IR protein levels (blue diamonds), IR activation [pIR$^{(Tyr1162/1163)}$, green triangles], IRS1 protein levels (red triangles), IRS1 inactivation [pIRS1$^{(Ser307)}$, brown squares] and IRS1 activation [pIRS1$^{(Tyr632)}$, black dots] evaluated in the hippocampus of WT mice at 3 ($n=6$), 6 ($n=6$), 12 ($n=6$) and 18 ($n=6$) months of age. Upper panels: western blot analyses. Representative bands are shown. Lower panels: densitometric analyses of western blot protein bands. Protein levels were normalized per total protein load. IR- and IRS1-associated phosphorylations were normalized by taking into account the respective protein levels and are expressed as the ratio between the phosphorylated form and the total protein levels: pIR$^{(Tyr1162/1163)}$/IR, pIRS1$^{(Ser307)}$/IRS1 and pIRS1$^{(Tyr632)}$/IRS1. Densitometric values shown are given as percentage of 3 months-old mice set as 100%. Means $\pm$ SEM, *$p < 0.05$, **$p < 0.01$ and ***$p < 0.001$ vs 3 months; †$p < 0.05$ and †††$p < 0.001$ vs 6 months; ‡$p < 0.05$ vs 12 months (ANOVA with post hoc Turkey t-test). (For interpretation of the references to color in this figure legend, the reader is referred to the web version of this article.)

overcame BIR *in vitro*, was associated with a remarkable increase of BVR-A Tyr phosphorylation (Fig. 6A). Finally, we found that BIR also parallels a significant reduction of the BVR-A reductase activity (Fig. 6D). All together these observations suggest that BIR is associated with a decreased BVR-A activation, and that this phenomenon could be overwhelmed by higher doses of insulin, which, instead, promote an increase of BVR-A activation and IRS1 Tyr phosphorylation.

3.7. Increased oxidative and nitrosative stress levels promote BVR-A impairment and BIR in SH-SY5Y neuroblastoma cells

Since the elevation of the oxidative and nitrosative stress levels is associated with both reduced BVR-A Tyr phosphorylation and BIR during AD and normal aging in mice, we evaluated the effects produced by a nitrosative agent (ONOO$^-$, 50–500 μM for 24 h) or a pro-oxidant agent (H$_2$O$_2$, 0–50 μM for 24 h), on SH-SY5Y neuroblastoma cells with the aim to unravel whether oxidative/nitrosative stress could be a cause of the observed BVR-A impairment and BIR. Indeed, ONOO$^-$ treatment was associated with a significant elevation of IR protein levels at all the doses tested, whereas a decrease of IR activation at 250 and 500 μM was observed (see Supplementary Fig. 4). Furthermore, ONOO$^-$ promoted a significant increase of IRS1 inhibition both at 250 and 500 μM (Fig. 6B). In addition to that, ONOO$^-$ at the same doses led to a reduction of BVR-A protein levels (see Supplementary Fig. 4) and activation (Fig. 6B).

Treatment with H$_2$O$_2$ did not produce changes of IR protein levels, while it led to increased IR activation at both 10 μM and 50 μM (see Supplementary Fig. 5). In addition, a decrease of IRS1 protein levels and an enhanced IRS1 inhibition at the same doses is observable (see Supplementary Fig. 5). Furthermore, 50 μM H$_2$O$_2$ promoted significantly increased BVR-A protein levels (see Supplementary Fig. 5). Because 50 μM H$_2$O$_2$ did recapitulate our previous observation in human AD brain and results from 3xTg-AD mice, in which elevated oxidative stress levels co-exist with increased BVR-A protein levels and BIR, we then analyzed BVR-A activation in this condition. Interestingly, 50 μM H$_2$O$_2$ for 24 h led to a consistent decrease of BVR-A Tyr phosphorylation (Fig. 6B).

In accordance with findings in human and mice, we found that both ONOO$^-$ and H$_2$O$_2$ at the highest doses promote a significant reduction of BVR-A reductase activity (Fig. 6D).

These evidence clearly suggests that increased oxidative and nitrosative stress levels finally promote a reduction of BVR-A activation and BIR. Intriguingly, increased nitrosative stress levels could be among the mechanisms responsible for the observed reduction of BVR-A protein levels and activation in the early phases of AD pathology in 3xTg-AD mice and probably also in WT mice with age.

3.8. Lack of BVR-A promotes BIR in SH-SY5Y neuroblastoma cells

Given that (i) BIR is associated with a reduced BVR-A activation and that (ii) both increased oxidative and nitrosative stress levels promote a decrease of BVR-A activation, we evaluated the effects produced on IR and IRS1 by BVR-A knockdown in SH-SY5Y neuroblastoma cells.

Interestingly, the silencing of BVR-A (siRNA) was associated with reduced IR protein levels and increased IR activation (Fig. 7). Despite of that, a clear inactivation of IRS1 was observed (Fig. 7). To note, the effects produced by insulin in cells in which BVR-A was silenced consistently differ from those produced under normal conditions. Indeed, we observed a dramatic increase of IRS1 inhibition following insulin, which is even higher compared to siRNA alone (Fig. 7). These results indicate that reduced BVR-A activation, here mimicked by knocking-down the protein, leads to

BIR, and that the effect normally produced by insulin would be shifted toward a condition of BIR when BVR-A does not function properly.

3.9. BVR-A impairment causes BIR through mTOR

Based on our hypothesis that reduced BVR-A activation would favor IRS1 hyper-activation, which is then turned-off through specific feed-back mechanisms, we then focused our attention on the mammalian target of rapamycin (mTOR). Indeed, once persistently stimulated, mTOR is able to phosphorylate IRS1 on Ser residues critical for BIR, including Ser307 [19,42] and previous studies from both our groups [43,44] and others [45–48] reported about the hyper-activation of mTOR in AD.

Therefore, we first evaluated mTOR protein levels and activation (measured by the levels of Ser2448 phosphorylation), in SH-SY5Y neuroblastoma cells treated with insulin, to investigate whether also in our cellular model the BIR was associated with mTOR hyper-activation. We found that insulin treatment does not promote significant changes with regard to mTOR protein levels or activation (see Supplementary Fig. 6A). Interestingly, by re-challenging pre-treated cells with increasing doses of insulin (0.1–5 μM for 1 h), we observed a significant further increase of mTOR with insulin 0.1 μM and 0.5 μM and a subsequent decrease at the doses of 1 μM and 5 μM (see Supplementary Fig. 6A). These changes parallel either BIR or IRS1 activation and are consistent with changes of BVR-A activation in the same cells (Fig. 6A and see Supplementary Fig. 3).

Furthermore, to better clarify the impact of increased oxidative/nitrosative stress levels and BVR-A reduction on mTOR activation, we evaluated the effects produced by ONOO$^-$, H$_2$O$_2$ or BVR-A silencing in SH-SY5Y neuroblastoma cells. Interestingly, although ONOO$^-$ and H$_2$O$_2$ treatments dose-dependently increased mTOR protein levels (see Supplementary Figs. 6B and C) they produced different outcomes on mTOR activation. Indeed, in accordance with previous findings [49], ONOO$^-$ promoted a decrease of mTOR phosphorylation (see Supplementary Fig. 6B), whereas a consistent elevation of p-mTOR^{Ser2448} with 50 μM H$_2$O$_2$ was observed (see Supplementary Fig. 6C). Surprisingly, in a subsequent set of experiments, the knock-down of BVR-A was associated with a strong activation of mTOR (see Supplementary Fig. 7), while was further elevated in cells treated with both BVR-A siRNA and 0.1 μM insulin for 24 h (see Supplementary Fig. 7). To note, H$_2$O$_2$-induced elevation of p-mTOR^{Ser2448} is concomitant with the inactivation of BVR-A (Fig. 5C) and the increased IRS1 Ser307 phosphorylation levels in the same samples (Fig. 6C).

To check whether also in our mice BIR was associated with mTOR hyper-activation we then analyzed changes occurring both as effect of AD pathology and normal aging. We found that 3xTg-AD mice are characterized by a significant elevation of p-mTOR$^{(Ser2448)}$ at 12 months (Fig. 8A), which is consistent with increased pIRS1$^{(Ser307)}$ levels observed at this age (Fig. 3C). Furthermore, changes associated with normal aging processes highlight that following a reduction of mTOR activity from 3 to 12 months a significant increase at 18 months of age occurs with respect to both 6 and 12 months (Fig. 8B). Although the extent of mTOR phosphorylation at 18 months is still lower than those observed at 3 months of age, we think that in consideration of the reduction observed at both 6 and 12 months of age, the raise found at 18 months could be responsible at least in part of IRS1 inactivation. Indeed, in terms of percentage, this increase occurs at a similar extent of those observed in 3xTg-AD mice or SH-SY5Y neuroblastoma cells characterized by BIR.

Taken together, these findings denote that increased mTOR activation parallels either BVR-A impairment or insulin resistance in mice and cells, thus strengthening our hypothesis that
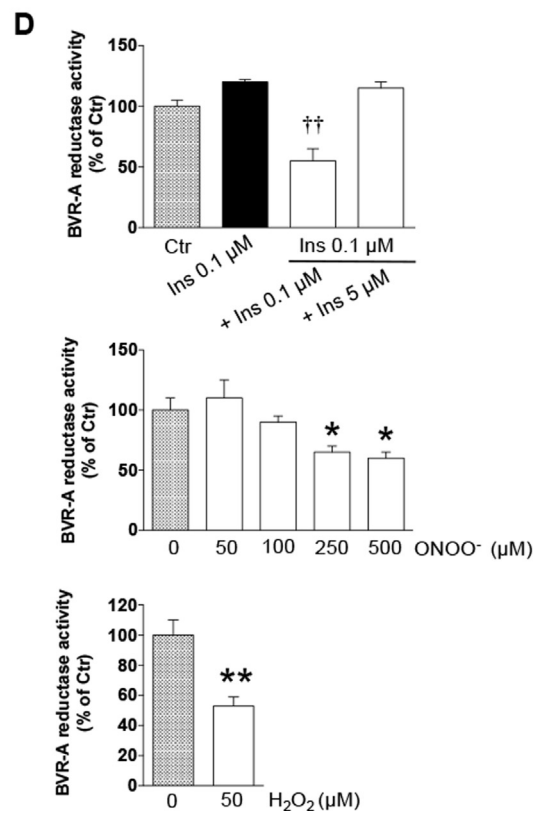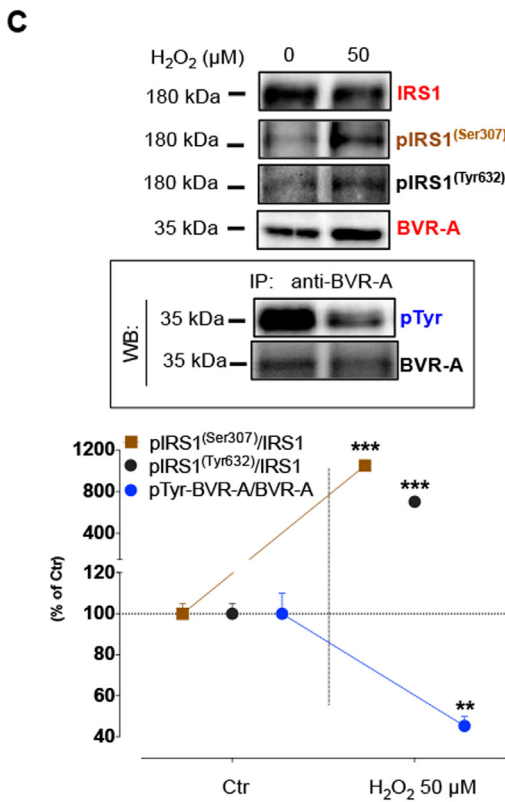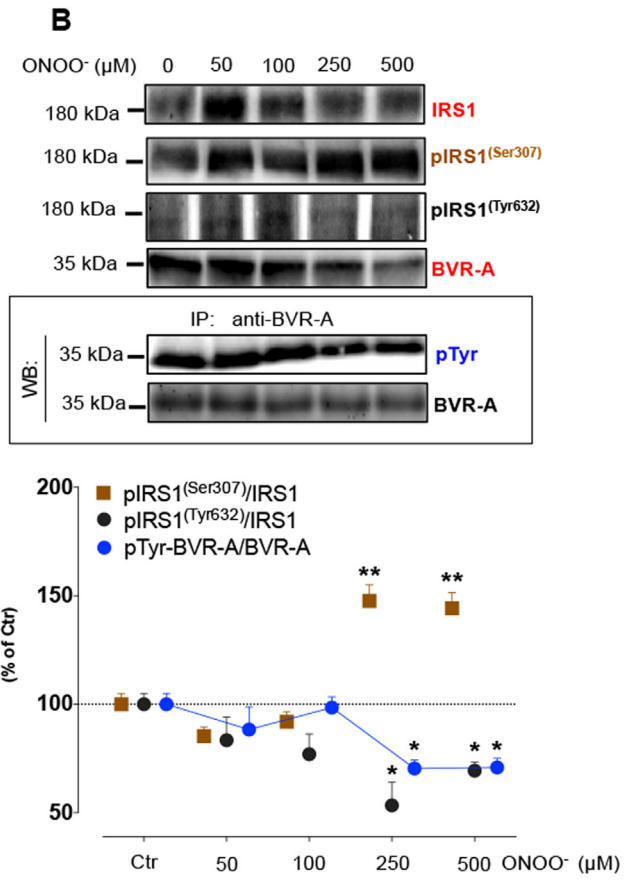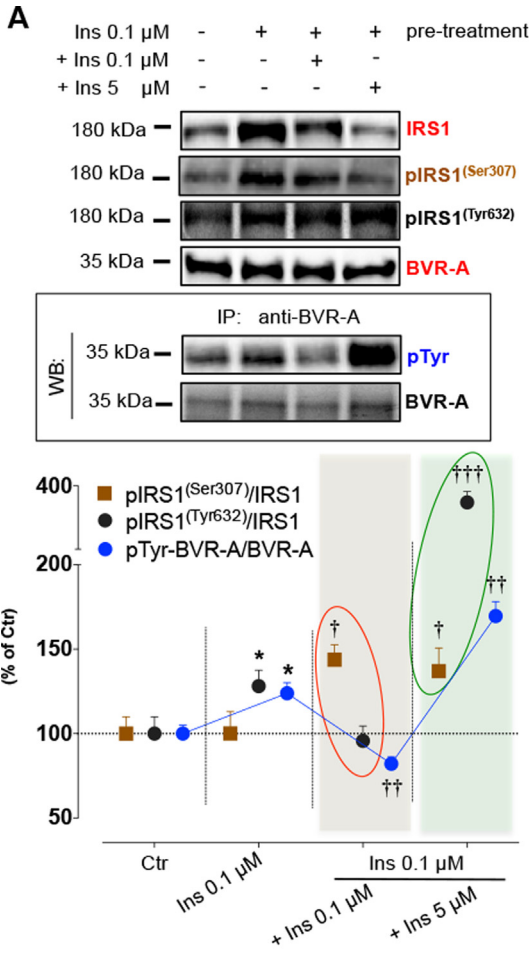
dysregulation of BVR-A would lead to IRS1 hyperactivation, which is then turned-off by feed-back mechanism(s) including mTOR. Once again, the effects produced by nitrosative stress could be prominent in the early phase of the pathology or the aging process, whereas a major effect of oxidative stress is evident later.

4. Discussion

The onset of BIR in AD is a matter still under debate because the complexity of the mechanisms underlying this phenomenon [50,51,52]. Interestingly, causes of peripheral insulin resistance in obesity or T2DM such as the activation of adaptive feedback/feed-forward mechanisms responsible for the inhibition of IRS1 have been also found in AD. One of the most conceivable pathway suggests that Aβ oligomers, from one side, promote the down-regulation of plasma membrane IR [16] whereas, from the other side, lead to the activation of neuronal tumor necrosis factor-alpha (TNF-α) receptor and the aberrant activation of stress-regulated kinases [i.e. Jun N-terminal kinase (JNK), I kappa B kinase (IKK), and protein kinase R (PKR)] [17,18,53] and endoplasmic reticulum (ER) stress (PKR-mediated phosphorylation of eIF2α-P) [18], which leads to IRS1 inactivation. The above-mentioned proteins are all down-stream effectors shared by a number of signaling pathways (i.e. lipid metabolism and inflammation) and thus not exclusively related to the insulin signaling, although IRS1 is among their substrates [19].

Given that, BIR appears to be an event secondary to the activation of these kinases due to other mechanisms including the elevation of the oxidative/nitrosative stress levels [54], inflammatory processes and ER stress [17,18]. However, none of the identified mechanisms has been characterized so far in terms of age-associated changes finally culminating with the onset of the BIR in AD.

The novelty of our work is to provide for the first time evidence (i) about a dysfunction of insulin signaling produced by the impairment of a member of the signaling itself, i.e., BVR-A, and (ii) on how the identified mechanism develops with AD pathology and normal aging in mice.

BVR-A is a unique protein characterized by the ability to carry out two kinds of activities: the "reductase" activity and the "Ser/Thr/Tyr kinase" activity through which BVR-A regulates cell signaling and gene expressions (reviewed in [24]). These two activities are differently modulated since the phosphorylation of specific Tyr residues (Tyr$^{198/228/291}$) promoted by IR is required for the activation of its kinase activity [22], whereas the auto-phosphorylation of specific Ser/Thr residues regulates the reductase activity [35]. Interestingly, Ser/Thr auto-phosphorylation is independent from Tyr phosphorylation [22]. Instead, Tyr phosphorylation is critical for BVR-A mediated IRS1 phosphorylation [22].

The involvement of BVR-A in the insulin signaling is indeed fascinating for two main reasons: BVR-A, as IRS1, is a direct target of IR kinase activity and once IR-phosphorylated is able to phosphorylate IRS1 on Ser residues [human(h)/mouse(m) hSer^{307}/mSer^{302}, hSer^{312}/mSer^{307} and hSer^{616}/mSer^{612}] critical for insulin signaling [22]; and (ii) BVR-A contains specific motifs in its sequence through which they possibly modulates IR kinase activity both negatively and positively [27].

Recent studies from the Butterfield group demonstrated increased BVR-A protein levels in the hippocampus of both AD and aMCI subjects [21], possibly due to elevated oxidative/nitrosative stress levels [55]. The first surprising evidence of this work is the unexpected reduced BVR-A protein levels found in the hippocampus of 3xTg-AD mice aged from 3 to 12 months of age, with respect to WT controls (Fig. 2A–C). Besides, increased BVR-A protein levels have been found only at 18 months of age, in the presence of robust AD pathology (see Fig. 1B) [56]. Interestingly, reduction of BVR-A protein levels, already evident at 3 months, seems to be a specific event, which occurs independently of TNF-α elevation (Fig. 4) and prior Aß and Tau accumulation (Fig. 1B).

To further understand if the reduction of BVR-A protein levels was a peculiarity of this protein, we also evaluated the expression of its partner HO-1, normally increased following the elevation of the oxidative/nitrosative stress levels [57] and co-expressed with BVR-A in brain regions that express these enzymes under normal conditions [58]. Surprisingly, HO-1 protein levels do not change from 3 to 12 months while they are significantly increased at 18 months in the hippocampus of 3xTg-AD mice (see Supplementary Fig. 8), thus strengthening the idea that reduction of BVR-A protein levels could be peculiar of earlier stages of AD contributing to its onset and development.

Furthermore, data about BVR-A activation state allowed us to identify three different phases along the progression of AD pathology in 3xTg-AD mice: a first phase at 3 months of age characterized by an increased BVR-A Tyr phosphorylation, a second phase at 6 months of age during which we observed a drastic decrease of BVR-A activation, and a third phase (12–18 months) characterized by a consistent increase of BVR-A nitration. These results, while reinforced human data [18 months of age, increased protein levels and 3-NT modifications], on the other side clearly highlight an early impairment of BVR-A activation starting at 6 months of age (Fig. 2). Noticeable, reduced BVR-A activation is first due to reduced Tyr residues phosphorylation (Fig. 2B), rather than increased 3-NT modifications, which becomes consistent at 12 months (Fig. 2C). One conceivable explanation is that increased total 3-NT levels observed at 6 months (Fig. 1A) affect redox-sensitive signaling pathways, such as phosphorylation cascades [59] and data obtained on cells treated with ONOO⁻ reinforced this hypothesis. Indeed, both phosphorylation and nitration reactions share the same target residues, i.e., Tyr residues, and are mutually exclusive events [60]. BVR-A reductase activity appear to be significantly reduced only at 12 months of age when increased

Fig. 6. BVR-A impairment is associated with BIR in SH-SY5Y neuroblastoma cells. (A) Insulin 0.1 μM for 24 h induced both IRS1 activation (pIRS1$^{(Tyr632)}$, black dots) and BVR-A activation (pTyr-BVR-A, blue dots) in SH-SY5Y neuroblastoma cells thus mirroring the physiological insulin signaling. Instead, pre-treated cells further treated with insulin (0.1 or 5 μM) for an additional hour to mimic insulin over-exposure, showed dose-dependent effects. Indeed, insulin 0.1 μM was associated with BIR (increased pIRS1$^{(Ser307)}$, brown squares) and BVR-A inactivation, whereas insulin 5 μM treatment by-passed BIR and was associated with increased activation of both IRS1 and BVR-A. *$p < 0.05$, vs Ctr; †$p < 0.05$, ††$p < 0.01$ and †††$p < 0.001$ vs Ins 0.1 μM (ANOVA with post hoc Tukey t-test). (B) ONOO⁻ (50-500 μM) for 24 h dose-dependenlty promoted BIR (increased pIRS1$^{(Ser307)}$, brown squares) and BVR-A inactivation (reduced pTyr-BVR-A, blue dots) in SH-SY5Y neuroblastoma cells. Decreased pIRS1$^{(Tyr632)}$ was also observed. *$p < 0.05$ and **$p < 0.01$ vs Ctr (ANOVA ANOVA with post hoc Tukey t-test). (C) H$_2$O$_2$ 50 μM for 24 h promoted BIR (increased pIRS1$^{(Ser307)}$, brown squares) and BVR-A inactivation (reduced pTyr-BVR-A, blue dots) in SH-SY5Y neuroblastoma cells. Increased pIRS1$^{(Tyr632)}$ was also observed, but IRS1 inactivation overcomes this effect. *$p < 0.05$, vs Ctr (Student's t-test). (D) BVR-A reductase activity relative to A, B and C evaluated as described in Materials and Methods and expressed as percent of Ctr ($n=3$ independent cultures/group). Means ± SEM, *$p < 0.05$ and **$p < 0.01$ vs Ctr mice; †$p < 0.05$, vs Ins 0.1 μM (ANOVA with post hoc Tukey t-test for Ins and ONOO⁻ related experiments; Student's t-test for H$_2$O$_2$ related experiment). For A, B and C: Upper panels: western blot analyses. Representative bands are shown. Lower panels: densitometric analyses of western blot protein bands. Protein levels were normalized per total protein load. IR- and IRS1-associated phosphorylations were normalized by taking into account the respective protein levels and are expressed as the ratio between the phosphorylated form and the total protein levels: pIR$^{(Tyr1162/1163)}$/IR, pIRS1$^{(Ser307)}$/IRS1 and pIRS1$^{(Tyr632)}$/IRS1. pTyr levels on BVR-A were normalized by using total BVR-A as loading control [35,36].Densitometric values shown are given as percentage of control cells (Ctr) set as 100%. Means ± SEM ($n=3$ independent cultures/group). (For interpretation of the references to color in this figure legend, the reader is referred to the web version of this article.)
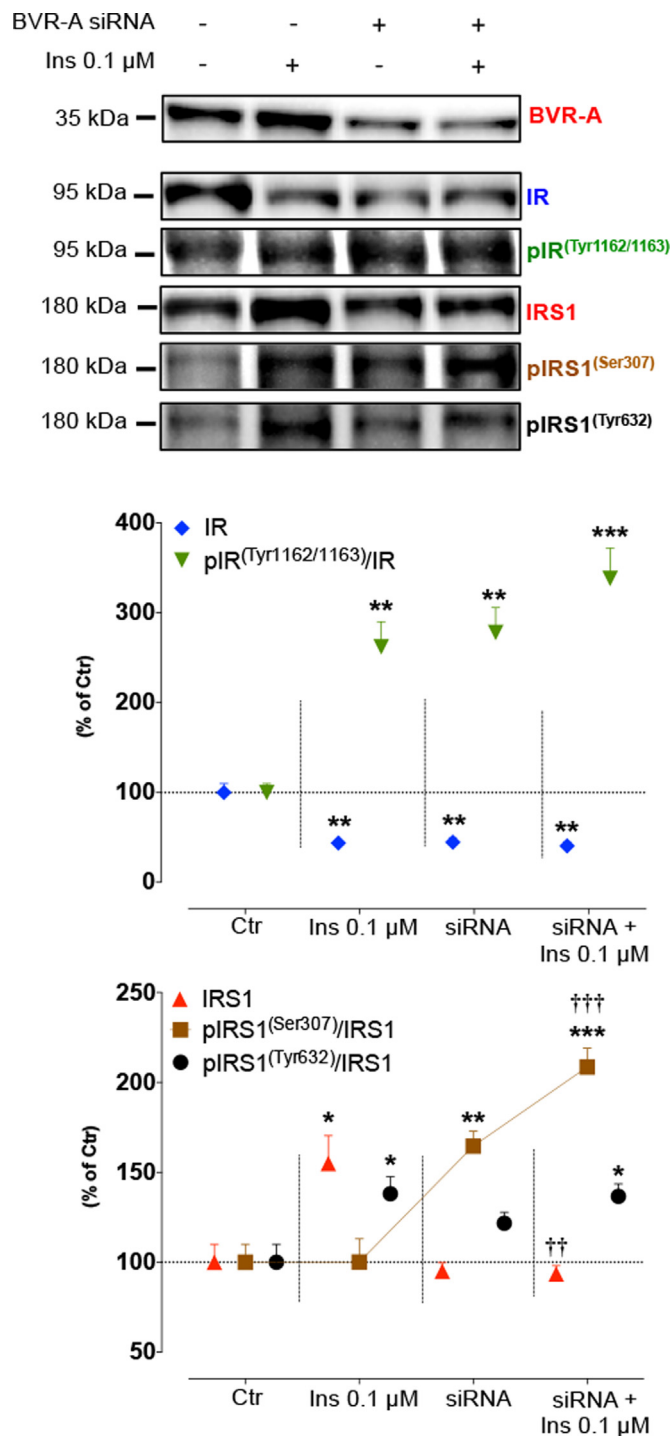
Fig. 7. Lack of BVR-A promotes BIR in SH-SY5Y neuroblastoma cells. Silencing BVR-A with a specific siRNA for 24 h was associated with IR activation (increased pIR$^{(Tyr1162/1163)}$/IR ratio, green triangles) but promoted BIR (increased pIRS1$^{(Ser307)}$, brown squares) in SH-SY5Y neuroblastoma cells. Insulin 0.1 μM was not able to promote the activation of the insulin signaling, but, rather, worsened BIR in cells lacking BVR-A. Increased pIRS1$^{(Tyr632)}$ was also observed, but IRS1 inactivation overcomes this effect. *$p < 0.05$, **$p < 0.01$ and ***$p < 0.001$ vs Ctr; †$p < 0.05$, ††$p < 0.01$ and †††$p < 0.001$ vs Ins 0.1 μM (ANOVA with post hoc Tukey t-test). Upper panels: western blot analyses. Representative bands are shown. Lower panels: densitometric analyses of western blot protein bands. Protein levels were normalized per total protein load. IR- and IRS1-associated phosphorylations were normalized by taking into account the respective protein levels and are expressed as the ratio between the phosphorylated form and the total protein levels: pIR$^{(Tyr1162/1163)}$/IR, pIRS1$^{(Ser307)}$/IRS1 and pIRS1$^{(Tyr632)}$/IRS1. Densitometric values shown are given as percentage of control cells (Ctr) set as 100%. Means ± SEM ($n=3$ independent cultures/group). (For interpretation of the references to color in this figure legend, the reader is referred to the web version of this article.)

levels of 3-NT modifications are clearly evident (Fig. 2), thus suggesting that increased oxidative/nitrosative stress levels promote the impairment of both BVR-A activities with the progression of AD pathology.

Given that picture, results about IR and IRS1 activation are intriguing and contribute to shed light on the molecular mechanisms underlying BIR in AD. According to our hypothesis, the hippocampus of 3xTg-AD mice is first characterized by an increased IR and IRS1 activation from 3 to 6 months followed by reduction of IR activation together with a consistent IRS1 inactivation starting at 12 months of age (Fig. 3), these latter events coherent with human data [9]. These two phases agree with changes of BVR-A activation state. Indeed, while at 3 months of age it is conceivable that IR hyper-activation could be blunted by increased BVR-A activation, which would avoid IRS1 hyper-activation (Figs. 2A and 3A), at 6 months of age reduced BVR-A activation is associated with IRS1 hyper-activation (Figs. 2B and 3B). At 12 and 18 months of age, the persistent inactivation of BVR-A is associated with a marked increase of IRS1 inactivation, and thus BIR (Figs. 2C–D and 3C–D). We propose that the period included between 6 and 12 months of age is critical and represents the time frame for the switch from activated insulin signaling to BIR in the hippocampus of 3xTg-AD mice. Interestingly, previous studies reported about a hyper-metabolic state in the brain of 7-month-old 3xTg-AD mice in contrast to the hypo-metabolic state observed at 13 months [61]. Similarly, increased glucose uptake in young mice, followed by decreased uptake and reduced glucose transporter (GLUT)-4 levels (the only GLUT being insulin sensitive in the brain) in old 3xTg-AD mice have been reported [63,64]. Although brain glucose uptake is mainly insulin-independent [65], insulin signaling alterations might alter depolarization-induced glucose uptake via other pathways as observed also in AD subjects [9,66]. Furthermore, impairment of cognitive functions in 3xTg-AD mice deteriorate dramatically in 3xTg-AD mice from 6 to 12 months of age [56]. Considering that insulin signaling positively modulate synaptic plasticity and long-term potentiation (LTP) [67,68], our data on the impairment of the insulin signaling mainly occurring in the same time-frame, support a role of defective insulin signaling in the decline of cognitive functions [56]. All these changes parallel peripheral signs of insulin resistance including a progressive (1) plasma glucose intolerance, (2) increase of plasma insulin levels, (3) reduction of fasting insulin and (4) hyperglycemia from 6 to 14 months [62]. Indeed, while raising peripheral insulin levels acutely elevates brain and cerebrospinal fluid insulin levels, prolonged peripheral hyper-insulinemia down-regulates insulin receptors and thus insulin sensitivity into the brain [54,69,70].

Another striking finding of the current research, is the observation that BIR occurs in the hippocampus of WT mice with normal aging and is associated with reduced BVR-A protein levels and increased BVR-A 3-NT modifications (Fig. 5A–B). However, it is evident that a reduction of BVR-A protein levels at 12 months of age precedes the appearance of the BIR at 18 months (Fig. 5A–B). In that picture, data about TNF-α levels only partially explain the observed changes. Indeed, whether increased TNF-α levels could contribute to BVR-A reduction at 12 months (see Supplementary Fig. 2C and Fig. 5A) [39], reduced TNF-α levels at 18 months would not explain neither the persistent reduction of BVR-A protein levels nor the huge increase of IRS1 phosphorylation (see Supplementary Fig. 2C and Fig. 5A–B). However, what emerges from our data is that, also during normal aging, BIR parallels increased oxidative/nitrosative stress levels (see Supplementary Fig. 2B) and BVR-A impairment (Fig. 5A–B). These results strengthen the role of BVR-A in the onset of BIR and we propose the impairment of BVR-A as a bridge connecting aging and AD.

From a molecular point of view our cell-based experiments clearly highlight that BIR is associated with a reduction of BVR-A

activation and that oxidative and nitrosative stress promotes BIR and BVR-A inactivation. These results extend previous findings showing that reducing BVR-A activation improves glucose uptake in HEK293A cells [22]. Considering that the regulation of glucose uptake and energy metabolism in the central nervous system differs from peripheral tissues and that insulin mainly exerts neurotrophic functions [8,65,71], we demonstrated that silencing BVR-A in neurons promotes IRS1 inactivation and negatively impacts the effects produced by insulin itself (Fig. 7).

We hypothesize that persistent inactivation of BVR-A could

promote BIR by feedback mechanisms causing IRS1 inhibitory phosphorylation. Among putative kinases, a pivotal role is played by mTOR. Intriguingly, recent data suggest the hyperactivation of mTOR is involved in the neurodegenerative process, including AD and Down Syndrome [43–48,72]. In agreement with these findings, we showed the aberrant activation of mTOR either following insulin over-exposure or H_2O_2 treatment. Instead, $ONOO^-$ treatment was associated with a reduction of mTOR activation, which could explain the results obtained in young mice undergoing AD neuropathology or aging characterized by increased total 3-NT levels (Figs 2A and Supplementary 2B).

Noteworthy, the silencing of BVR-A is associated with mTOR hyper-activation (see Supplementary Fig. 7). However, whether the observed increased mTOR activation is a direct effect of BVR-A or is the results of the sustained activation of the insulin signaling has to be clarified. The fact that BVR-A also could regulate mTOR as it does with other kinases [24] appear very fascinating in light of a previous report showing that high doses of biliverdin (the substrate of BVR-A) promote the activation of the mTOR pathway [73]. Since biliverdin is not a kinase itself and it is known to inhibit BVR-A expression [39], in light of our findings the effect of biliverdin on mTOR could be mediated by a down-regulation of BVR-A. The idea that following the reduction of BVR-A activation, the hyper-activation of mTOR could be one of the mechanisms responsible of IRS1 inactivation is confirmed by data obtained in mice both during AD-like pathology and normal aging. Indeed, mTOR hyper-activation occurs at 12 months of age in 3xTg-AD mice (Fig. 8A), exactly when we observed significant IRS1 inhibition (Fig. 3C), as well as in WT mice, but at 18 months of age (Figs. 8B and 5B).

Taken together, these observations extend the novelty of our work by elucidating mechanisms contributing to BIR in AD. Furthermore, considering previous findings proposing the elevation of TNF-α as mediator of BIR in AD [18], and based on our results in 3xTg-AD mice showing increased levels of TNF-α only at 18 months of age, we may hypothesize that the impairment of BVR-A, coupled with the hyper-activation of mTOR, are early events contributing to BIR.

Finally, another interesting result of our study is the observation that high doses of insulin (5 μM), administered to SH-SY5Y neuroblastoma cells previously stimulated with insulin 0.1 μM, are able to overcomes BIR (Fig. 6A). This effect is associated with the increased activation of BVR-A (Fig. 6A) and the reduction of p-mTOR to control levels (see Supplementary Fig. 6A). Intriguingly, it is likely that the effectiveness of therapeutic strategies proposing intranasal insulin administration to slow/improve AD pathology [74] could involve BVR-A. Such studies are in progress in our groups.
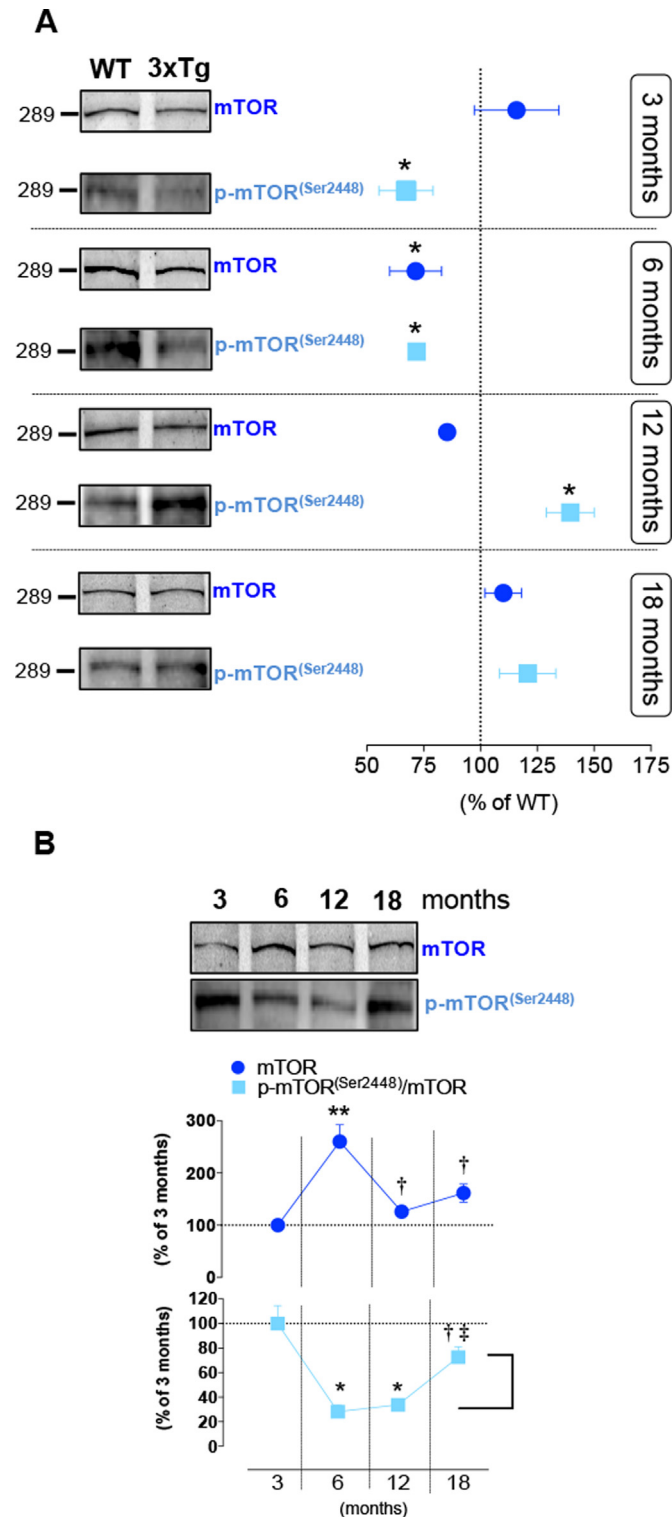
Fig. 8. Hyper-activation of mTOR parallels BIR both during AD and normal aging. (A) mTOR protein levels (blue dots) and activation [p-mTOR(Ser2448), blue squares] evaluated in the hippocampus of 3xTg-AD mice at 3 ($n=6$), 6 ($n=6$), 12 ($n=6$), and 18 ($n=6$) months of age. *Left panels:* western blot analyses. Representative bands are shown. *Right panels:* densitometric analyses of western blot protein bands. Protein levels were normalized per total protein load. mTOR phosphorylation was normalized per total mTOR protein levels and is expressed as p-mTOR(Ser2448)/mTOR ratio. Densitometric values shown are given as percentage of WT mice ($n=6$/group) set as 100%. Means ± SEM, $*p < 0.05$, vs WT mice (Student's t-test). (B) mTOR protein levels (blue dots) and activation [p-mTOR(Ser2448), blue squares] evaluated in the hippocampus of WT mice as effect of normal aging at 3 ($n=6$), 6 ($n=6$), 12 ($n=6$), and 18 ($n=6$) months of age. *Upper panels:* western blot analyses. Representative bands are shown. *Lower panels:* densitometric analyses of western blot protein bands. Protein levels were normalized per total protein load. mTOR phosphorylation was normalized per total mTOR protein levels and is expressed as p-mTOR(Ser2448)/mTOR ratio. Densitometric values shown are given as percentage of 3 months-old mice set as 100%. Means ± SEM, $*p < 0.05$ and $**p < 0.01$ vs 3 months; $†p < 0.05$ vs 6 months; $‡p < 0.05$ vs 12 months (ANOVA with post hoc Tukey t-test). (For interpretation of the references to color in this figure legend, the reader is referred to the web version of this article.)
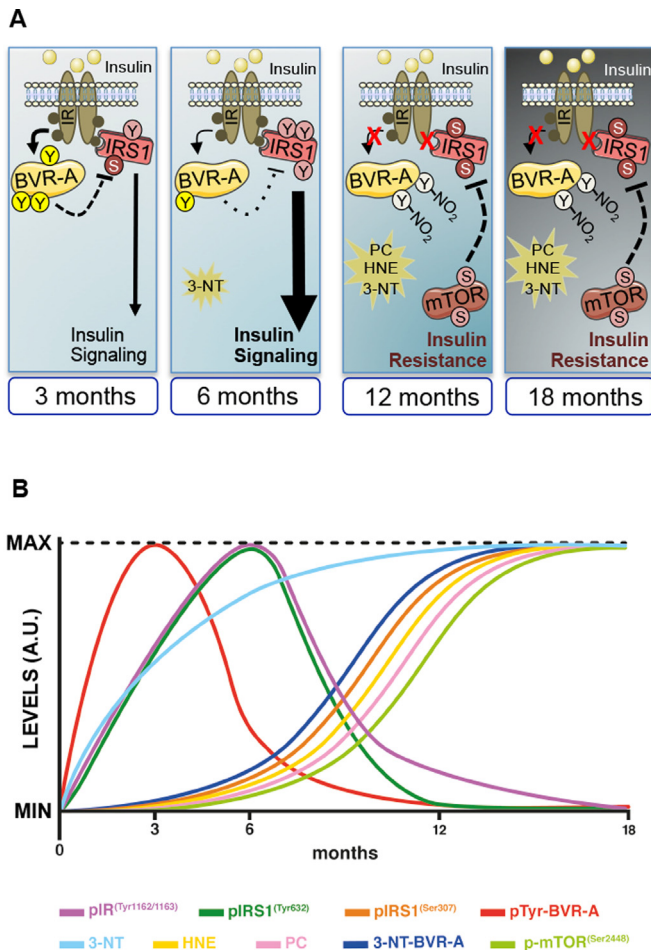
Fig. 9. Temporal profile of the events promoting BIR in the hippocampus 3xTg-AD mice. (A) Proposed mechanism leading to BIR in AD. At 3 months of age the insulin binding to IR promotes IR phosphorylation on Tyr residues, which leads to a consistent activation of BVR-A. This latter, in turn, probably blunts IRS1 hyper-activation thus allowing a still normal activation of the insulin signaling. At 6 months of age while IR appears to be still activated, BVR-A does not probably because increased 3-NT levels. Lacking BVR-A activity promotes IRS1 hyper-activation, which sustains the activation of the insulin signaling for a time perhaps longer than normal. Between 6 and 12 months of age, the further rise of the oxidative/nitrosative stress levels (PC, HNE and 3-NT) result in the oxidative stress-induced impairment of BVR-A, which contributes to maintain IRS1 hyperactive. IRS1 hyper-activation leads to the aberrant activation of mTOR, which through a feedback mechanism turn-off IRS1 thus leading to BIR. Finally, 18 months of age are characterized by the persistence of the same modifications observed at 12 months, which contribute to the maintenance of an BIR profile. Arrows, promotion; dotted lines, inhibition; Y, phosphor-Tyr residues; S, phospho-Ser residues; Y-NO₂, 3-NT modifications. (B) Temporal profile of the modifications occurring with regard to (i) IR, (ii) IRS1, (iii) BVR-A and (iv) mTOR activation diagrammed together with changes of oxidative/nitrosative stress markers.

5. Conclusion

In conclusion, we propose a new paradigm in which (i) increased oxidative/nitrosative stress levels would promote BVR-A impairment, (ii) BVR-A impairment would lead to IRS1 hyper-activation, because of the lack of the regulatory activity of BVR-A, (iii) IRS1 hyper-activation would sustain insulin signaling for a time longer than normal, thus activating feedback mechanisms, i.e., mTOR, turning-off IRS1-associated downstream effects (Fig. 9). All these events underlie the existence of at least two different phases along the progression of AD pathology, which require to be addressed in humans to develop early potential therapeutic interventions.

Appendix A. Supplementary material

Supplementary data associated with this article can be found in the online version at 10.1016/j.freeradbiomed.2015.12.012.

References

[1] S.M. de la Monte, M. Tong, Brain metabolic dysfunction at the core of Alzheimer's disease, Biochem. Pharmacol. 88 (2014) 548–559.

[2] F.G. De Felice, Alzheimer's disease and insulin resistance: translating basic science into clinical applications, J. Clin. Investig. 123 (2013) 531–539.

[3] A. Ott, R.P. Stolk, F. van Harskamp, H.A. Pols, A. Hofman, M.M. Breteler, Diabetes mellitus and the risk of dementia: The Rotterdam Study, Neurology 53 (1999) 1937–1942.

[4] P.K. Crane, R. Walker, E.B. Larson, Glucose levels and risk of dementia, New. Engl. J. Med. 369 (2013) 1863–1864.

[5] A.A. Willette, B.B. Bendlin, E.J. Starks, A.C. Birdsill, S.C. Johnson, B.T. Christian, O.C. Okonkwo, A. La Rue, B.P. Hermann, R.L. Koscik, E.M. Jonaitis, M.A. Sager, S. Asthana, Association of Insulin Resistance With Cerebral Glucose Uptake in Late Middle-Aged Adults at Risk for Alzheimer Disease, JAMA Neurol. 72 (2015) 1013–1020.

[6] J. Janson, T. Laedtke, J.E. Parisi, P. O'Brien, R.C. Petersen, P.C. Butler, Increased risk of type 2 diabetes in Alzheimer disease, Diabetes 53 (2004) 474–481.

[7] S. Craft, Alzheimer disease: Insulin resistance and AD–extending the translational path, Nat. Rev. Neurol. 8 (2012) 360–362.

[8] R. Ghasemi, A. Haeri, L. Dargahi, Z. Mohamed, A. Ahmadiani, Insulin in the brain: sources, localization and functions, Mol. Neurobiol. 47 (2013) 145–171.

[9] K. Talbot, H.Y. Wang, H. Kazi, L.Y. Han, K.P. Bakshi, A. Stucky, R.L. Fuino, K. R. Kawaguchi, A.J. Samoyedny, R.S. Wilson, Z. Arvanitakis, J.A. Schneider, B. A. Wolf, D.A. Bennett, J.Q. Trojanowski, S.E. Arnold, Demonstrated brain insulin resistance in Alzheimer's disease patients is associated with IGF-1 resistance, IRS-1 dysregulation, and cognitive decline, J. Clin. Investig. 122 (2012) 1316–1338.

[10] E. Blazquez, E. Velazquez, V. Hurtado-Carneiro, J.M. Ruiz-Albusac, Insulin in the brain: its pathophysiological implications for States related with central insulin resistance, type 2 diabetes and Alzheimer's disease, Front. Endocrinol. 5 (2014) 161.

[11] J.M. Horwood, F. Dufour, S. Laroche, S. Davis, Signalling mechanisms mediated by the phosphoinositide 3-kinase/Akt cascade in synaptic plasticity and memory in the rat, Eur. J. Neurosci. 23 (2006) 3375–3384.

[12] V. Calabrese, C. Mancuso, M. Calvani, E. Rizzarelli, D.A. Butterfield, A.M. Stella, Nitric oxide in the central nervous system: neuroprotection versus neurotoxicity, Nat. Rev. Neurosci. 8 (2007) 766–775.

[13] K. Akter, E.A. Lanza, S.A. Martin, N. Myronyuk, M. Rua, R.B. Raffa, Diabetes mellitus and Alzheimer's disease: shared pathology and treatment? Br. J. Clin. Pharmacol. 71 (2011) 365–376.

[14] E. Steen, B.M. Terry, E.J. Rivera, J.L. Cannon, T.R. Neely, R. Tavares, X.J. Xu, J. R. Wands, S.M. de la Monte, Impaired insulin and insulin-like growth factor expression and signaling mechanisms in Alzheimer's disease–is this type 3 diabetes? J. Alzheimer's Dis.: Jad. 7 (2005) 63–80.

[15] E.J. Rivera, A. Goldin, N. Fulmer, R. Tavares, J.R. Wands, S.M. de la Monte, Insulin and insulin-like growth factor expression and function deteriorate with progression of Alzheimer's disease: link to brain reductions in acetylcholine, J. Alzheimer's Dis.: Jad. 8 (2005) 247–268.

[16] F.G. De Felice, M.N. Vieira, T.R. Bomfim, H. Decker, P.T. Velasco, M.P. Lambert, K. L. Viola, W.Q. Zhao, S.T. Ferreira, W.L. Klein, Protection of synapses against Alzheimer's-linked toxins: insulin signaling prevents the pathogenic binding of Abeta oligomers, Proc. Natl. Acad. Sci. United S. Am. 106 (2009) 1971–1976.

[17] T.R. Bomfim, L. Forny-Germano, L.B. Sathler, J. Brito-Moreira, J.C. Houzel, H. Decker, M.A. Silverman, H. Kazi, H.M. Melo, P.L. McClean, C. Holscher, S. E. Arnold, K. Talbot, W.L. Klein, D.P. Munoz, S.T. Ferreira, F.G. De Felice, An anti-diabetes agent protects the mouse brain from defective insulin signaling caused by Alzheimer's disease- associated Abeta oligomers, J. Clin. Investig. 122 (2012) 1339–1353.

[18] M.V. Lourenco, J.R. Clarke, R.L. Frozza, T.R. Bomfim, L. Forny-Germano, A. F. Batista, L.B. Sathler, J. Brito-Moreira, O.B. Amaral, C.A. Silva, L. Freitas-Correa, S. Espirito-Santo, P. Campello-Costa, J.C. Houzel, W.L. Klein, C. Holscher, J. B. Carvalheira, A.M. Silva, L.A. Velloso, D.P. Munoz, S.T. Ferreira, F.G. De Felice, TNF-alpha mediates PKR-dependent memory impairment and brain IRS-1 inhibition induced by Alzheimer's beta-amyloid oligomers in mice and monkeys, Cell. Metab. 18 (2013) 831–843.

[19] K.D. Copps, M.F. White, Regulation of insulin sensitivity by serine/threonine phosphorylation of insulin receptor substrate proteins IRS1 and IRS2, Diabetologia 55 (2012) 2565–2582.

[20] E. Barone, F. Di Domenico, G. Cenini, R. Sultana, R. Coccia, P. Preziosi, M. Perluigi, C. Mancuso, D.A. Butterfield, Oxidative and nitrosative modifications of biliverdin reductase-A in the brain of subjects with Alzheimer's disease and amnestic mild cognitive impairment, J. Alzheimer's Dis.: Jad. 25 (2011) 623–633.

[21] E. Barone, F. Di Domenico, G. Cenini, R. Sultana, C. Cini, P. Preziosi, M. Perluigi, C. Mancuso, D.A. Butterfield, Biliverdin reductase–a protein levels and activity in the brains of subjects with Alzheimer disease and mild cognitive impairment, Biochim. Et. Biophys. Acta 1812 (2011) 480–487.

[22] N. Lerner-Marmarosh, J. Shen, M.D. Torno, A. Kravets, Z. Hu, M.D. Maines, Human biliverdin reductase: a member of the insulin receptor substrate family with serine/threonine/tyrosine kinase activity, Proc. Natl. Acad. Sci. U.S.A. 102 (2005) 7109–7114.

[23] B. Wu, X. Liu, J. Shen, Old biliverdin reductase: links to insulin resistance and may be a novel therapeutic target, Med. Hypotheses 71 (2008) 73–76.

[24] J. Kapitulnik, M.D. Maines, Pleiotropic functions of biliverdin reductase: cellular signaling and generation of cytoprotective and cytotoxic bilirubin, Trends Pharmacol. Sci. 30 (2009) 129–137.

[25] R. Stocker, Antioxidant activities of bile pigments, Antioxid. Redox Signal 6 (2004) 841–849.

[26] E. Barone, S. Trombino, R. Cassano, A. Sgambato, B. De Paola, E. Di Stasio, N. Picci, P. Preziosi, C. Mancuso, Characterization of the S-denitrosylating activity of bilirubin, J. Cell. Mol. Med. 13 (2009) 2365–2375.

[27] P.E. Gibbs, N. Lerner-Marmarosh, A. Poulin, E. Farah, M.D. Maines, Human biliverdin reductase-based peptides activate and inhibit glucose uptake through direct interaction with the kinase domain of insulin receptor, FASEB J. 28 (2014) 2478–2491.

[28] E. Barone, F. Di Domenico, C. Mancuso, D.A. Butterfield, The Janus face of the heme oxygenase/biliverdin reductase system in Alzheimer disease: it's time for reconciliation, Neurobiol. Dis. 62 (2014) 144–159.

[29] S. Oddo, A. Caccamo, J.D. Shepherd, M.P. Murphy, T.E. Golde, R. Kayed, R. Metherate, M.P. Mattson, Y. Akbari, F.M. LaFerla, Triple-transgenic model of Alzheimer's disease with plaques and tangles: intracellular Abeta and synaptic dysfunction, Neuron 39 (2003) 409–421.

[30] T. Cassano, A. Romano, T. Macheda, R. Colangeli, C.S. Cimmino, A. Petrella, F. M. LaFerla, V. Cuomo, S. Gaetani, Olfactory memory is impaired in a triple transgenic model of Alzheimer disease, Behav. Brain Res. 224 (2011) 408–412.

[31] A. Romano, L. Pace, B. Tempesta, A.M. Lavecchia, T. Macheda, G. Bedse, A. Petrella, C. Cifani, G. Serviddio, G. Vendemiale, S. Gaetani, T. Cassano, Depressive-like behavior is paired to monoaminergic alteration in a murine model of Alzheimer's disease, Int. J. Neuropsychopharmacol. 18 (2015).

[32] T. Cassano, G. Serviddio, S. Gaetani, A. Romano, P. Dipasquale, S. Cianci, F. Bellanti, L. Laconca, A.D. Romano, I. Padalino, F.M. LaFerla, F. Nicoletti, V. Cuomo, G. Vendemiale, Glutamatergic alterations and mitochondrial impairment in a murine model of Alzheimer disease, Neurobiol. aging 33 (2012) e1121–1112.

[33] C.M. Mayer, D.D. Belsham, Central insulin signaling is attenuated by long-term insulin exposure via insulin receptor substrate-1 serine phosphorylation, proteasomal degradation, and lysosomal insulin receptor degradation, Endocrinology 151 (2010) 75–84.

[34] G. Cenini, R. Sultana, M. Memo, D.A. Butterfield, Effects of oxidative and nitrosative stress in brain on p53 proapoptotic protein in amnestic mild cognitive impairment and Alzheimer disease, Free. Radic. Biol. Med. 45 (2008) 81–85.

[35] M. Salim, B.A. Brown-Kipphut, M.D. Maines, Human biliverdin reductase is autophosphorylated, and phosphorylation is required for bilirubin formation, J. Biol. Chem. 276 (2001) 10929–10934.

[36] N. Lerner-Marmarosh, T. Miralem, P.E. Gibbs, M.D. Maines, Human biliverdin reductase is an ERK activator; hBVR is an ERK nuclear transporter and is required for MAPK signaling, Proc. Natl. Acad. Sci. U.S.A. 105 (2008) 6870–6875.

[37] F. Di Domenico, E. Barone, C. Mancuso, M. Perluigi, A. Cocciolo, P. Mecocci, D. A. Butterfield, R. Coccia, HO-1/BVR-a system analysis in plasma from probable Alzheimer's disease and mild cognitive impairment subjects: a potential biochemical marker for the prediction of the disease, J. Alzheimer's Dis.: Jad. 32 (2012) 277–289.

[38] S. Oddo, A. Caccamo, B. Tseng, D. Cheng, V. Vasilevko, D.H. Cribbs, F.M. LaFerla, Blocking Abeta42 accumulation delays the onset and progression of tau pathology via the C terminus of heat shock protein70-interacting protein: a mechanistic link between Abeta and tau pathology, J. Neurosci. 28 (2008) 12163–12175.

[39] P.E. Gibbs, T. Miralem, M.D. Maines, Characterization of the human biliverdin reductase gene structure and regulatory elements: promoter activity is enhanced by hypoxia and suppressed by TNF-alpha-activated NF-kappaB, FASEB J. 24 (2010) 3239–3254.

[40] M.C. Janelsins, M.A. Mastrangelo, S. Oddo, F.M. LaFerla, H.J. Federoff, W. J. Bowers, Early correlation of microglial activation with enhanced tumor necrosis factor-alpha and monocyte chemoattractant protein-1 expression specifically within the entorhinal cortex of triple transgenic Alzheimer's disease mice, J. Neuroinflammation 2 (2005) 23.

[41] S. Zaheer, R. Thangavel, Y. Wu, M.M. Khan, D. Kempuraj, A. Zaheer, Enhanced expression of glia maturation factor correlates with glial activation in the brain of triple transgenic Alzheimer's disease mice, Neurochem. Res. 38 (2013) 218–225.

[42] C.J. Carlson, M.F. White, C.M. Rondinone, Mammalian target of rapamycin regulates IRS-1 serine 307 phosphorylation, Biochem. Biophys. Res. Commun. 316 (2004) 533–539.

[43] M. Perluigi, G. Pupo, A. Tramutola, C. Cini, R. Coccia, E. Barone, E. Head, D. A. Butterfield, F. Di Domenico, Neuropathological role of PI3K/Akt/mTOR axis in Down syndrome brain, Biochim. Et. Biophys. Acta 1842 (2014) 1144–1153.

[44] A. Tramutola, J.C. Triplett, F. Di Domenico, D.M. Niedowicz, M.P. Murphy, R. Coccia, M. Perluigi, D.A. Butterfield, Alteration of mTOR signaling occurs early in the progression of Alzheimer disease (AD): analysis of brain from subjects with pre-clinical AD, amnestic mild cognitive impairment and late-stage AD, J. Neurochem. 133 (2015) 739–749.

[45] A. Caccamo, S. Majumder, A. Richardson, R. Strong, S. Oddo, Molecular interplay between mammalian target of rapamycin (mTOR), amyloid-beta, and Tau: effects on cognitive impairments, J. Biol. Chem. 285 (2010) 13107–13120.

[46] A. Caccamo, M.A. Maldonado, S. Majumder, D.X. Medina, W. Holbein, A. Magri, S. Oddo, Naturally secreted amyloid-beta increases mammalian target of rapamycin (mTOR) activity via a PRAS40-mediated mechanism, J. Biol. Chem. 286 (2011) 8924–8932.

[47] S. Oddo, The role of mTOR signaling in Alzheimer disease, Front Biosci. 4 (2012) 941–952.

[48] J. Bove, M. Martinez-Vicente, M. Vila, Fighting neurodegeneration with rapamycin: mechanistic insights, Nat. Rev. Neurosci. 12 (2011) 437–452.

[49] D.N. Tripathi, R. Chowdhury, L.J. Trudel, A.R. Tee, R.S. Slack, C.L. Walker, G. N. Wogan, Reactive nitrogen species regulate autophagy through ATM-AMPK-TSC2-mediated suppression of mTORC1, Proc. Natl. Acad. Sci. U.S.A. 110 (2013) E2950–E2957.

[50] F.G. De Felice, M.V. Lourenco, S.T. Ferreira, How does brain insulin resistance develop in Alzheimer's disease? Alzheimer's Dement.: J. Alzheimer's Assoc. 10 (2014) S26–S32.

[51] B. Cholerton, L.D. Baker, S. Craft, Insulin, cognition, and dementia, Eur. J. Pharmacol. 719 (2013) 170–179.

[52] G. Bedse, F. Di Domenico, G. Serviddio, T. Cassano, Aberrant insulin signaling in Alzheimer's disease: current knowledge, Front. Neurosci. 9 (2015) 204.

[53] Q.L. Ma, F. Yang, E.R. Rosario, O.J. Ubeda, W. Beech, D.J. Gant, P.P. Chen, B. Hudspeth, C. Chen, Y. Zhao, H.V. Vinters, S.A. Frautschy, G.M. Cole, Beta-amyloid oligomers induce phosphorylation of tau and inactivation of insulin receptor substrate via c-Jun N-terminal kinase signaling: suppression by omega-3 fatty acids and curcumin, J. Neurosci. 29 (2009) 9078–9089.

[54] D.A. Butterfield, F. Di Domenico, E. Barone, Elevated risk of type 2 diabetes for development of Alzheimer disease: a key role for oxidative stress in brain, Biochim. Et. Biophys. Acta 1842 (2014) 1693–1706.

[55] S. Corrao, P. Santalucia, C. Argano, C.D. Djade, E. Barone, M. Tettamanti, L. Pasina, C. Franchi, T. Kamal Eldin, A. Marengoni, F. Salerno, M. Marcucci, P. M. Mannucci, A. Nobili, R. Investigators, Gender-differences in disease distribution and outcome in hospitalized elderly: data from the REPOSI study, Eur. J. Intern. Med. 25 (2014) 617–623.

[56] R. Medeiros, M.A. Chabrier, F.M. LaFerla, Elucidating the triggers, progression, and effects of Alzheimer's disease, J. Alzheimer's Dis.: Jad. 33 (Suppl 1) (2013) S195–S210.

[57] R. Gozzelino, V. Jeney, M.P. Soares, Mechanisms of cell protection by heme oxygenase-1, Annu. Rev. Pharmacol. Toxicol. 50 (2010) 323–354.

[58] J.F. Ewing, C.M. Weber, M.D. Maines, Biliverdin reductase is heat resistant and coexpressed with constitutive and heat shock forms of heme oxygenase in brain, J. Neurochem. 61 (1993) 1015–1023.

[59] H.P. Monteiro, Signal transduction by protein tyrosine nitration: competition or cooperation with tyrosine phosphorylation-dependent signaling events? Free. Radic. Biol. Med. 33 (2002) 765–773.

[60] D.A. Butterfield, E.R. Stadman, Protein oxidation processes in aging brain, in: S. T. Paula, E.E. Bittar (Eds.), Advances in Cell Aging and Gerontology, 1997, pp. 161–191.

[61] H. Sancheti, I. Patil, K. Kanamori, R. Diaz Brinton, W. Zhang, A.L. Lin, E. Cadenas, Hypermetabolic state in the 7-month-old triple transgenic mouse model of Alzheimer's disease and the effect of lipoic acid: a 13C NMR study, J. Cereb. blood Flow. Metab. 34 (2014) 1749–1760.

[62] M. Vandal, P.J. White, G. Chevrier, C. Tremblay, I. St-Amour, E. Planel, A. Marette, F. Calon, Age-dependent impairment of glucose tolerance in the 3xTg-AD mouse model of Alzheimer's disease, FASEB J. 29 (2015) 4273–4284.

[63] H. Sancheti, G. Akopian, F. Yin, R.D. Brinton, J.P. Walsh, E. Cadenas, Age-dependent modulation of synaptic plasticity and insulin mimetic effect of lipoic acid on a mouse model of Alzheimer's disease, PLOS One 8 (2013) e69830.

[64] R.M. Nicholson, Y. Kusne, L.A. Nowak, F.M. LaFerla, E.M. Reiman, J. Valla, Regional cerebral glucose uptake in the 3xTG model of Alzheimer's disease highlights common regional vulnerability across AD mouse models, Brain Res.

1347 (2014) 179–185.

[65] J. Jurcovicova, Glucose transport in brain-effect of inflammation, Endocr. Regul. 48 (2014) 35–48.

[66] A. Klip, The many ways to regulate glucose transporter 4, Appl. Physiol., Nutr., Metab. 34 (2009) 481–487.

[67] R. Nistico, V. Cavallucci, S. Piccinin, S. Macri, M. Pignatelli, B. Mehdawy, F. Blandini, G. Laviola, D. Lauro, N.B. Mercuri, M. D'Amelio, Insulin receptor beta-subunit haploinsufficiency impairs hippocampal late-phase LTP and re-cognition memory, Neuromolecular Med. 14 (2012) 262–269.

[68] L.P. van der Heide, A. Kamal, A. Artola, W.H. Gispen, G.M. Ramakers, Insulin modulates hippocampal activity-dependent synaptic plasticity in a N-methyl-d-aspartate receptor and phosphatidyl-inositol-3-kinase-dependent manner, J. Neurochem. 94 (2005) 1158–1166.

[69] M.W. Schwartz, D.F. Figlewicz, S.E. Kahn, D.G. Baskin, M.R. Greenwood, D. Porte Jr., Insulin binding to brain capillaries is reduced in genetically obese, hyperinsulinemic Zucker rats, Peptides 11 (1990) 467–472.

[70] B.J. Wallum, G.J. Taborsky Jr., D. Porte Jr., D.P. Figlewicz, L. Jacobson, J.C. Beard, W.K. Ward, D. Dorsa, . Cerebrospinal fluid insulin levels increase during in-travenous insulin infusions in man, J. Clin. Endocrinol. Metab. 64 (1987) 190–194.

[71] M. Belanger, I. Allaman, P.J. Magistretti, Brain energy metabolism: focus on astrocyte-neuron metabolic cooperation, Cell. Metab. 14 (2011) 724–738.

[72] A.M. Iyer, J. van Scheppingen, I. Milenkovic, J.J. Anink, H. Adle-Biassette, G. G. Kovacs, E. Aronica, mTOR Hyperactivation in down syndrome hippocampus appears early during development, J. Neuropathol. Exp. Neurol. 73 (2014) 671–683.

[73] K. Bisht, B. Wegiel, J. Tampe, O. Neubauer, K.H. Wagner, L.E. Otterbein, A. C. Bulmer, Biliverdin modulates the expression of C5aR in response to en-dotoxin in part via mTOR signaling, Biochem. Biophys. Res. Commun. 449 (2014) 94–99.

[74] S. Craft, L.D. Baker, T.J. Montine, S. Minoshima, G.S. Watson, A. Claxton, M. Arbuckle, M. Callaghan, E. Tsai, S.R. Plymate, P.S. Green, J. Leverenz, D. Cross, B. Gerton, Intranasal insulin therapy for Alzheimer disease and amnestic mild cognitive impairment: a pilot clinical trial, Arch. Neurol. 69 (2012) 29–38.